universität wien

DIPLOMARBEIT

The Role of Class I Histone Deacetylases in Cardiac Development of Chicken Embryos

Claudia Engelmaier

angestrebter akademischer Grad

Magistra der Naturwissenschaften (Mag.rer.nat.)

Wien, 2011

Studienkennzahl lt. Studienblatt:	A 442
Studienrichtung lt. Studienblatt:	Diplomstudium Anthropologie
Betreuerin / Betreuer:	Ao. Univ.-Prof. Mag.rer.nat. Mag.phil. Dr.rer.nat. Sylvia Kirchengast

Contents

Abstract

Histone deacetylases (HDACs) are a family of enzymes regulating the acetylation level of histones as well as non-histone proteins and, thus, controlling gene activity. HDACs remove acetyl groups from histone tails, thereby acting as co-repressors of gene transcription. The functions of HDACs have been extensively studied in vitro and suggest important roles of HDACs in differentiation processes in vivo and in embryonic development in particular. However, the role of the different classes of HDACs in controlling developmental processes remains to be fully elucidated. In particular, our knowledge of the functions of class I HDACs (HDACs 1, 2, 3, and 8) during development is limited. This study has addressed the role of class I HDACs in cardiac development of the avian model organism “chicken” during early embryonic stages. Heart development is a complex and precisely controlled developmental process. Because of this complexity, the heart is the organ system with the highest congenital malformation rate in humans. In most cases, the role of class I HDACs during cardiac development has so far been inferred by analysis of conditional knock-out mice showing multiple heart malformations at birth. Due to a previously published study, the temporal expression patterns of HDACs 1, 2, 3, and 8 in the chick heart are known. Thus, to gain insight into the activities of class I HDACs in cardiac tissue, these enzymes were inhibited by Trichostatin A (TSA), a chemical inhibitor of HDACs. The inhibitor was applied to the hearts by implantation of acrylic beads soaked in TSA or by direct injection into the pericardial cavity. Subsequent histological and morphometric analysis, a proliferation assay (BrdU assay) as well as an apoptosis assay (TUNEL assay), and the determination of the acetylation level in the chick hearts by Western analysis allowed first insights into phenotypic effects of class I HDAC inhibition in avian cardiac tissue. The examined chicken hearts treated with the HDAC inhibitor displayed a range of severe phenotypes, such as atrial hypertrophy, ventricular hypertrophy, hypertrophy of the right ventricle, malformations of the ventricular septum, and aberrant formation of the outflow tract. However, the cardiac tissue showing hypertrophic effects, especially atrial hypertrophy, was found to be more pronounced than the other phenotypes. These findings offer a basis for further functional analysis of class I HDACs in cardiac development. Additionally, this study presents experimentations which were performed in embryonic chicken hearts for the first time; hopefully this piece of work provides possibilities for the development of novel manipulation procedures regarding the model system “chicken”.

Zusammenfassung

Histondeacetylasen (HDACs) sind eine Familie von Enzymen, die den Acetylierungslevel von Histonen und auch anderen Proteinen regulieren und so die Genaktivität kontrollieren. HDACs entfernen Acetylgruppen von Histonschwänzen, weswegen sie als Co-Repressoren der Gentranskription agieren. Die Funktionen von HDACs wurden ausführlich in vitro studiert und es wird angenommen, dass HDACs in in vivo Differenzierungsprozessen und im Speziellen in der Embryonalentwicklung eine wichtige Rolle spielen. Die Rollen der verschiedenen Klassen von HDACs in der Kontrolle von Entwicklungsprozessen müssen aber noch vollständig aufgeklärt werden. Insbesondere unser Wissen über die Funktionen von Klasse I HDACs (HDACs 1, 2, 3 und 8) während der Entwicklung ist begrenzt. Diese Studie hat die Rolle von Klasse I HDACs in der Herzentwicklung des Modellorganismus „Huhn“ während früher embryonaler Stadien zum Thema. Die Herzentwicklung ist ein komplexer und präzise gesteuerter Entwicklungsprozess. Aufgrund dieser Komplexität ist das Herz beim Menschen das Organsystem mit der höchsten Rate an angeborenen Missbildungen. In den meisten Fällen wurde die Rolle von Klasse I HDACs während der Herzentwicklung bisher anhand von Analysen konditioneller Knock-out Mäuse, die bei der Geburt mehrere Herzfehler zeigten, interpretiert. Durch eine vor Kurzem publizierte Studie sind die zeitlichen Expressionsmuster der HDACs 1, 2, 3 und 8 im Hühnerherzen bekannt. Um Einblicke in die Aktivitäten von Klasse I HDACs im Herzgewebe zu gewinnen, wurden diese Enzyme durch Trichostatin A (TSA), einem chemischen HDAC-Hemmer, inhibiert. Der Inhibitor wurde durch die Implantation von in TSA getränkten Acrylbeads oder durch direkte Injektion in die Perikardhöhle in das Herz eingebracht. Die nachfolgende histologische und morphometrische Analyse, ein Proliferationsassay (BrdU-Assay) als auch ein Apoptoseassay (TUNEL-Assay) und die Bestimmung des Acetylierungslevels in den Hühnerherzen durch eine Western-Analyse erlaubte erste Einblicke in phänotypische Effekte, die durch Hemmung der Klasse I HDACs im Herzgewebe von Vögeln entstanden sind. Die untersuchten Hühnerherzen, die mit dem HDAC inhibitor behandelt wurden, zeigten eine Reihe von schweren Phänotypen, wie atriale Hypertrophie, ventrikuläre Hypertrophie, Hypertrophie des rechten Ventrikels, Fehlbildungen des Ventrikelseptums und aberrante Formation des Ausflusstraktes. Die Herzen, die hypertrophe Effekte zeigten, insbesondere jene mit atrialer Hypertrophie, waren ausgeprägter als die anderen Phänotypen. Diese Ergebnisse bieten eine Basis für weitere funktionelle Analysen von Klasse I HDACs in der Herzentwicklung. Außerdem präsentiert diese Studie

Experimente, die am embryonalen Hühnerherzen das erste Mal durchgeführt wurden; diese Arbeit soll Möglichkeiten für die Entwicklung neuer Manipulationsverfahren im Hinblick auf das Modellsystem „Huhn“ bieten.

1. Introduction

1.1. The epigenetic mark

Every multicellular organism consists of a considerable number of various cell types, each of them displaying a unique profile of gene expression which can be altered in response to physiological signals being caused by environmental influences. The modification of gene expression patterns is strongly affected by transcriptional regulation; transcriptional regulatory factors bind reversibly to amino-acid residues within histone tails changing chromatin structure and therefore regulating gene transcription. The effect can be an activating one or a repressive one. (Allis et al., 2009; Haberland et al., 2008)

Histones are alkaline proteins consisting, as all other proteins do, of amino acids. These proteins are organized in two super-families: core histones (H2A, H2B, H3, and H4) and linker histones (H1 and H5). The four core histones form a so called histone octamer comprising of two H2A-H2B dimers and one H3-H4 tetramer; around each octamer 147 base pairs of DNA are wrapped forming a nucleosome. The linker histone H1 is associated to the nuclesome and binds to the entry and exit sites of the DNA securing it into place, thus enabling higher order structures.

The four core histones are highly conserved through evolution and share a comparably similar structure, including a so called histone tail protruding from the N- or amino terminus of the protein. The histone tail holds several possibilities of being covalently modified; it is the site of posttranslational modifications. (Allis et al., 2009)

The most widespread posttranslational modifications include methylation, phosphorylation and acetylation (Strahl & Allis, 2000); such modifications enable, like mentioned above, environment-cell interaction via linking extracellular signals with the genome (Allis et al., 2009; Haberland et al., 2008).

The collaboration of several histone modifications is implied to establish a so called “histone code” which expands the one-dimensionality of the primary DNA sequence; as a result the functional plasticity of the eukaryotic genome is increased. (Jenuwein & Allis, 2001)

1.1.1. Histone acetylation and deacetylation

Histone acetylation and deacetylation are contradictory processes; they regulate gene transcription by locally altering the electric charge of the histone, thereby affecting the

chromatin structure and the accessibility for the transcription machinery (Allis et al., 2009; Gregoretti et al., 2004).

For the histones being destined to pack the negatively charged DNA into chromatin, the surface of the proteins is rich with amino acids containing side chains with a positive charge, like lysine and arginine. Concerning acetylation, there were only found acetylated lysines up to now (Allis et al., 2009). If lysine residues within histone tails become acetylated, the positive charge of the amino acid is neutralized, hence, the attraction between the negative charge of the DNA and the positive charge of the histone is reduced and the structure of the chromatin relaxes; the accessibility for the transcription machinery to the target genes grows and the genes become activated (Brunmeir et al., 2009; Shahbazian & Grunstein, 2007). In addition, bromodomain proteins bind to acetylated histones and function as transcriptional activators (Ruthenburg et al., 2007).

On the contrary, the deacetylation of histones promotes the opposite effect; the elimination of acetyl moieties leads to chromatin condensation followed by repression of transcription (Brunmeir et al., 2009; Shahbazian & Grunstein, 2007).

1.1.2. Histone deacetylases influence gene expression

Histone acetylation and deacetylation are regulated by histone acetyltransferases (HATs) and histone deacetylases (HDACs). These two enzyme families act as antagonists; hence histone acetylation is a reversible process. HATs acetylate histone tails, therefore, locally opening the chromatin and enabling activation of target genes as described above. Considered as transcriptional co-repressors, HDACs act contradictory; they remove acetyl groups from histone tails (Allis et al., 2009; Brunmeir et al., 2009; Shahbazian & Grunstein, 2007) causing chromatin compaction and aggravated transcription (Allis et al., 2009; Murko et al., 2010; Shahbazian & Grunstein, 2007). Moreover, besides histones HDACs also deacetylate non-histone proteins like transcription factors (e. g. p53, E2F1, and YY1) and tubulin, a protein of the cellular cytoskeleton (Brunmeir et al., 2009).

In addition to their role in histone acetylation and deacetylation, both, HATs and HDACs, influence the affinity of acetyl-histone binding factors. These enzymes act as key factors of the regulatory mechanism for gene expression, playing a considerable role in the determination of the cell-fate of multicellular organisms during embryogenesis. (Murko et al., 2010)

HDACs are unable to bind directly to the DNA; their influence on the chromatin structure depends on their corroboration with chromatin-binding proteins like transcriptional activators and repressors which ensure the HDACs' recruitment to target genes. Another possibility to exert their influence is the anticipation of HDACs in multiprotein transcriptional complexes (Brunmeir et al., 2009; Haberland et al., 2008; Shahbazian & Grunstein, 2007); the specificity and biological reactions of HDAC recruitment depend on the assembly of the complex (Brunmeir et al., 2009). Hence, concerning the modulation and regulation of individual gene programmes displayed in defined cell types of multicellular organisms, the effect and specificity of HDACs correlate with the identity, the attainable binding partners and the signalling milieu of the cell (Haberland et al., 2008). Within such a multiprotein complex one task of HDACs may be the preparation of target genes; the acetyl marks have to be detached from the chromatin before new modifications (e. g. histone methylation) established by other proteins of the same complex, can take place (Brunmeir et al., 2009).

Inhibition or delition of *Hdacs* generally leads to up- or downregulation of gene expression (Haberland et al., 2008; Montgomery et al., 2007).

1.1.3. The HDAC superfamily

The HDAC superfamily is ancient and wide in range (Brunmeir et al., 2009; Haberland et al., 2008; Murko et al., 2010). The 11 classic HDACs encoded by the mammalian genome are categorized into three classes due to sequence similarities: class I (HDAC1, HDAC2, HDAC3, and HDAC8), class II (HDAC4, HDAC5, HDAC6, HDAC7, HDAC9, and HDAC10), and class IV (HDAC11-like). Moreover, the mammalian genome also encodes class III HDACs, which are also addressed as sirtuins; these are NAD-dependant Sir2-like acetylases derived from Saccharomyces cervisiae being functionally unrelated to the classic HDACs (Allis et al., 2009; Gregoretti et al., 2004).

Class II HDACs are reported to be separable into two subclasses: HDAC4, HDAC5, HDAC7, and HDAC9 are summarized as class IIa HDACs and class IIb contains HDAC6 and HDAC10 (Yang & Seto, 2008).

1.2. Class I HDACs

The class I HDAC family comprises of HDAC1, HDAC2, HDAC3, and HDAC8, which are expressed ubiquitously throughout the organism, primarily accumulated in the cell nuclei; these proteins demonstrate a high enzymatic activity towards histone substrates (Haberland et al., 2008; Murko et al., 2010).

All class I HDACs consist of an evolutionarily conserved catalytic domain which includes more than 300 amino acids; thus, this domain takes an extensive part of the protein (Brunmeir et al., 2009; Haberland et al., 2008). The catalytic domain is called histone deacetylase domain (HDAC domain). It is composed of a pocket holding certain charged and uncharged amino acids which interact with a zinc ion as a charge-relay system; hence, the HDAC domain is important for the enzymatic function of the protein. (Brunmeir et al., 2009)

In human HDAC 1 comprises of 482 amino acids; HDAC2 obtains 488 amino acids. HDACs 1 and 2 include a HDAC association domain (HAD) formed by the first ~50 amino acids of the N-terminus of the protein, which partly overlaps with the HDAC domain reaching from residues ~10 to ~320; the HAD is required for protein-protein interaction enabling homo- and heterodimerisation. (Brunmeir et al., 2009)

The C-terminal portion of class I HDACs is more specific and contains characteristic domains dependent on the HDAC isoform. HDAC1 includes a C-terminal nuclear localisation signal (NLS); in contrast, HDAC 2 holds a coiled-coil domain at its C-terminus for probable further protein-protein interaction. (Brunmeir et al., 2009)

HDAC3 consists of 428 amino acids in human. As in HDACs 1 and 2 the catalytic HDAC domain of HDAC3 is localized in the conserved N-terminal part of the protein reaching from amino acids 3 to 316 (Escaffit, 2007). The first 122 N-terminal residues of HDAC3 form a sequence which enables oligomerization of the protein with itself (Yang et al., 2002); this region seems to be crucial for cell viability of DT40 cells (Takami & Nakayama, 2000). The last 27 amino acids at the C-terminal end of HDAC3 are necessary for histone deacetylation and, consequently, for transcriptional repression. It is thought possible, that deletion of this C-terminally sequence alters the protein's global conformation and causes inactivity of the HDAC domain. Besides obtaining a NLS at its C-terminus, ranging from residues 313 to 428, HDAC3 also acquires a nuclear export signal (NES) which streches from amino acids 180 to 313; thus, HDAC 3 can be accumulated not only in the cell nucleus, but also in the cytoplasm. It is supposed that the equilibrium between the NLS and the NES is determined by the cell type and by environmental conditions. (Yang et al., 2002)

Human HDAC8 is composed of 377 amino acids. The central region of HDAC8, containing the catalytic domain with an NLS in its center, shows high similarity to the other class I HDACs; this part of the proteins is evolutionarily highly conserved. (Buggy et al., 2000; Hu et al., 2000; Van den Wyngaert et al., 2000) Conversely, amino acids 1 to 34 of the N-terminus and residues 348 to 377 of the C-terminus of HDAC8 are significantly distinct from the other members of the class I HDAC family; for these areas of the protein a specific role for HDAC8 is suggested (Van den Wyngaert et al., 2000). In addition, the C-terminal end of HDAC8 is shorter than the C-termini of HDACs 1 to 3 (Buggy et al., 2000). HDAC 8 includes a region containing mostly acidic amino acids (residues 83 to 95) which is not existent in the other class I HDACs; this domain is implied to be important for protein-protein interactions (Van den Wyngaert et al., 2000). For the expression of *Hdac8* in humans, two variants of transcripts were found (Buggy et al., 2000; Hu et al., 2000; Van den Wyngaert et al., 2000); concerning these transcripts differing in size, there are conflicting data: Buggy et al. (2000) detected transcripts of 1.7 kb and 2.4 kb, Hu and collegues (2000) observed 2.0 kb and 2.4 kb transcripts and Wyngaert et al. (2000) discovered RNA of 2.0 kb and 2.2 kb. These two RNA versions are suggested to be tissue-specific splice variants of HDAC8 (Van den Wyngaert et al., 2000) and are possibly playing a role in tumour cell lines (Buggy et al., 2000; Hu et al., 2000; Van den Wyngaert et al., 2000).

Futhermore, all class I HDACs are targets for posttranslational alterations themselves; modifications such as phosphorylation, acetylation and sumoylation are suggested to affect the stability of the protein, its enzymatic activity, nuclear import and the generation of complexes (Brunmeir et al., 2009).

HDAC1 and HDAC2 are built very similarly (Brunmeir et al., 2009; Haberland et al., 2008; Murko et al., 2010); in human they share 82% identity on the protein level; it is suggested that *Hdacs 1* and *2* are derived from a single ancestral gene which became duplicated within the vertebrate lineage (Brunmeir et al., 2009). The two enzymes mostly anticipate in repressive complexes like the Sin3 corepressor complex, the nucleosome remodelling and deacetylase complex (NuRD), the CoREST complex, the Polycomb repressive complex (PRC2) (Brunmeir et al., 2009; Haberland et al., 2008; Murko et al., 2010), the Nanog and Oct4 associated deacetylase complex (NODE), the SHIP1 containing complex (Brunmeir et al., 2009; Murko et al., 2010), and the BRAF-HDAC complex (BHC) together (Brunmeir et al., 2009).

With 34%-39% amino acid identity (Buggy et al., 2000; Hu et al., 2000; Van den Wyngaert et al., 2000), in human HDAC3 is most similar to HDAC8; hence, these both

proteins are evolutionary most closely related (Buggy et al., 2000; Hu et al., 2000). HDAC3 partly coincides with HDACs 1 and 2 as well: The HDAC3 sequence reaching from residues 181 to 333 was compared to the corresponding regions of HDAC1 and HDAC2; HDAC3 shares only ~68% identity with either HDAC1 or HDAC2. (Examining these corresponding sequences in HDACs 1 and 2, they yield 93% identity.) (Yang et al., 2002)
Additionally, HDAC3 can be detected in quite different complexes, such as the N-CoR-SMRT complex (Haberland et al., 2008; Murko et al., 2010) indicating specific biological functions of HDAC3 in comparison to the other members of class I HDACs (Murko et al., 2010).
Thus, HDACs 1, 2, and 3 can serve as catalytic subunits in multiprotein complexes cooperating with DNA sequence-specific transcription factors in order to inhibit transcription or interact with other chromatin modifying factors to form epigenetic programs (Murko et al., 2010).
Being phylogenetically analysed, HDAC8 was found to be a novel member of class I HDACs which can only be detected in vertebrates. The ancestral genes (orthologs) encoding for HDAC1-, HDAC2-, and HDAC3-like proteins already appear in Drosophila melanogaster. (Brunmeir et al., 2009)
Concerning the similarity of HDAC 8 to the other members of the class I HDAC family, there exist contradictory results for their relatedness in human: Buggy and colleagues (2000) suggest that HDAC8 and HDAC1 share 31% amino acid identity, with HDAC2 it shares 30% identity and 34% of the amino acid sequence of HDAC3 are identical to the sequence of HDAC8 (Buggy et al., 2000). Hu et al. (2000) propose 37% of HDAC8 to be identical with HDAC3, and with HDAC1 the protein shares as well 37% protein sequence identity (Hu et al., 2000). The laboratory of Van den Wyngaert et al. (2000) implies a 54% sequence similarity of HDAC8 to HDACs 1 and 2; with HDAC3 the enzyme shares 39% identity on the protein level (Van den Wyngaert et al., 2000).
For the anticipation of HDAC8 in a complex, there has been found no evidence so far (Haberland et al., 2008; Murko et al., 2010; Yang & Seto, 2008).

1.2.1. The role of class I HDACs during embryogenesis

The observation of all model systems studied so far showed results of expression of class I HDACs during most developmental stages in numerous different cell types.
Based on the evidence of being highly homologous, ubiquitously expressed, and being highly active towards common substrates, all class I HDACs are concluded to being

functionally redundant in vivo. Nevertheless, studies in knockout mice lacking *Hdac* genes showed that each single HDAC takes an individual part in the regulation of specific gene expression programs (Haberland et al., 2008; Murko et al., 2010).

In *Hdac1*-null mice Lagger et al. (2002) observed general growth retardation and serious proliferation defects leading to lethality before embryonic day 10.5 (E10.5) (Lagger et al., 2002). Furthermore, HDAC1 has been determined to target many genes playing a role in development and differentiation. Consequently, further examinations of the origin of *Hdac1*-null phenotypes are necessary. (Brunmeir et al., 2009)

Proliferation defects are also examined in embryonic stem cells lacking HDAC1; due to significantly decreased HDAC activity histones H3 and H4 become moderately hyperacetylated (Lagger et al., 2002; Zupkovitz et al., 2006) causing an upregulation of expression in about 4% of the genes, but also a downregulation in 3% of the genes. Subsequently, in embryonic stem cells HDAC1 is a vital deacetylase regulating individual gene expression profiles by activation or repression of specific promoters. (Zupkovitz et al., 2006)

Nevertheless, Montgomery et al. (2007) found out that a tissue-specific delition of *Hdac1* in the heart, brain and skeletal and smooth muscles is surprisingly well tolerated in the model system mouse. These findings are attributed to probable redundant effects of HDAC1 and HDAC2 (Montgomery et al., 2007).

In zebrafish a knockout of *hdac1* leads to lethal skeletal and neuronal defects (Nambiar et al., 2007).

Concerning *Hdac2*-null mice, two independently performed investigations maintained conflicting results. Montgomery et al. (2007) found that a global deletion of *Hdac2* in vivo resulted in perinatal affliction with severe cardiac defects leading to the death of the mice within the first 24 hours after birth. (Montgomery et al., 2007; Haberland et al., 2008; Murko et al., 2010) Hence, whereas *Hdac1*-null mice show an obvoius phenotype and early prenatal lethality, a global *Hdac2* delition causes no apparent phenotype in early development; however, the whole murine *Hdac2*-null offspring died within 24 h after birth (Montgomery et al., 2007). Therefore, it is suggested that HDAC1 particularly regulates a variety of essential target genes during embryogenesis or, supporting the redundancy thesis about HDACs 1 and 2 (described in the last paragraph of this chapter), that the quantity of expressed HDAC2 cannot compensate for the deficiency of HDAC1. Accordingly, in ES cells the expression level of HDAC1 is considerably higher than that of HDAC2 (Seiser, C., unpublished data). (Brunmeir et al., 2009)

In contrast to the complete lethality of *Hdac2*-null mice, Trivedi et al. (2007) found that mice being homozygous for a lacZ insertion in *Hdac2*, which was meant to generate a null mutation, showed a less severe phenotype: For half of the animals the gene disruption led to lethality within 25 days after birth. The other half of the mice, which survived, were smaller and and suffered from a lack of vitality and energy (lethargy); after 2 months they had recovered and developed normally. (Trivedi et al., 2007) Possibly varying genetic backgrounds of the tested mice in the 2 previously described studies provide an approach to these differing outcomes. Another feasible explanation would be that the lacZ insertion in *Hdac2* did not create a definite null allele but a hypomorphic allel; subsequently, *Hdac2* would be expressed sufficiently and enable viability. (Haberland et al., 2008; Murko et al., 2010)

In mice lacking HDAC3 in the germ line, defects in gastrulation induce a lethal embryonic phenotype dying by E9.5 (Montgomery et al., 2008).

A conditional deletion of *Hdac3* in the liver (Knutson et al., 2008) and the heart of a mouse embryo caused an increased lipid accumulation in these organs (Knutson et al., 2008; Montgomery et al., 2008). If the disrupted fatty-acid intake and metabolism concerned the heart, the mouse died after 3-4 months after birth (Montgomery et al., 2008).

In zebrafish the observation of morpholino-mediated knockdown of hdac3 mRNA showed disturbed formation and growth of the liver (Farooq et al., 2008).

Hdac8-null mice suffer from a highly specific deficiency of cranial neural crest cells causing skull instability, finally leading to perinatal lethality (Haberland et al., 2009).

HDAC1 and HDAC2 – working together or individually?

Sharing the highest similarity within class I HDACs, their proposed common ancestral origin and their joint participation in repressive multiprotein complexes, suggest redundant roles for HDACs 1 and 2. In contrast, several studies (as described above) report severe phenotypes after deletion of either *Hdac1* or *Hdac2* pointing to individual roles of the two enzymes in organisms containing both genes.

This implication is supported by a recent study reporting about spatially separated expression domains of *Hdac1* and *Hdac2* in the neural tube of a mouse embryo at stage E11.5. *Hdac1* expression was observed to be restricted to the inner ependymal layer of the neural tube (determined to become certain epithelial cells lining the brain ventricles and the central canal of the spinal cord), whereas transcripts of *Hdac2* were exclusively found in the middle cell layer, also called mantle layer (destined to generate the gray

matter of the CNS). (Murko et al., 2010) A current study about neuro-glial development in the CNS of the mouse conforms to these findings (MacDonald & Roskams, 2008). Thus, the preclusive *Hdac1* and *2* expression profiles in the central nervous system of the vertebrate model organism indicate that the two enzymes may act independently in specific cell-autonomous ways. Being ignorant to this suggestion, in mice with a specific deletion of either *Hdac1* or *Hdac2* in two different cell types of the CNS no distinct phenotype was observable; only a total lack of both enzymes affects death after birth. Taking all these findings into account, the suggestion of cross-regulation beyond the cell type has been arisen, however, to date remains to be elucidated. (Murko et al., 2010)

Occasionally, closer observations of the actions of the two HDACs in several mouse tissues and cell lines showed that a depleted expression level of one of both genes provoked a rise in the expression quantity of the other gene; the inactivation of *Hdac1* induces the upregulation of *Hdac2* expression and vice versa. Accordingly, the various phenotypes associated with either *Hdac1* or *Hdac2* deficiency are possibly caused by the increasing expression level of its paralog and not necessarily because of the silencing of the gene itself. (Brunmeir et al., 2009) Regarding this issue, Zupkovitz et al. (2006) performed gene expression studies in mouse ES cells; they found out that the effects of *Hdac1* deletion on the transcription of definite target genes can be quite inconsistent: In some cases HDAC2 cannot compensate for the loss of *Hdac1* expression, subsequently, the expression of numerous genes becomes induced. On the contrary, it is also possible that genes are transcriptionally repressed due to the escalated expression level and ectopic recruitment of HDAC2 to gene promoters. (Zupkovitz et al., 2006)

1.2.2. Cardiac functions and phenotypes of class I HDACs

As described in the previous chapter, a conditional deletion of *Hdac1* in the heart of a mouse embryo is well tolerated (Montgomery et al., 2007).

On the contrary, a global deletion of *Hdac2* in the same model organism causes lethality 24 hours or within 25 days after birth due to severe cardiac aberrations. Both laboratories (Montgomery et al., 2007; Trivedi et al., 2007) associated the observed obliteration of the right ventricular chamber due to uncontrolled proliferation of ventricular cardiomyocytes and the unusually slow heartbeat (bradycardia) with the postnatal death of the animals. (Montgomery et al., 2007; Trivedi et al., 2007)

Kook et al. (2003) demonstrated the interaction of HDAC2 with the homeodomain-only protein (HOP), which regulates cardiomyocyte proliferation and growth in an activating

or repressive way. They propose that HOP recruits HDAC2 to anticipate together in a repressive transcription complex controlling cardiac growth during mouse embryogenesis. The ability of HOP to associate with HDAC2 results in transcriptional repression of antihypertrophic genes; thus, overexpression of HOP induces cardiac hypertrophy (which means an escalated cell size for the same cell number) and fibrosis (i. e. the formation of additional fibrous connective tissue) leading to embryonic lethality. Overexpression of a mutant form of *Hop*, unable to recruit HDAC2, as well as HDAC inhibitors, as Trichostatin A (TSA), prevent hypertrophy of the heart. (Kook et al., 2003) Another possibility to weaken hypertrophic effects in cardiomyocytes is the deletion of *Hdac2*; although *Hop* was overexpressed, the examined murine hearts displayed no hypertrophy (Trivedi et al., 2007). In contrast, a tissue-specific overexpression of either *Hdac1* or *Hdac2* in the hearts of mice showed severe cardiac hypertrophy and dilatation resulting in sudden death of the animals (Montgomery et al., 2008; Trivedi et al., 2007).

Trying to find out, if the lethal phenotype of *Hdac2*-null mice demonstrates a cell-autonomous function of HDAC2 in cardiac myocytes, Montgomery and colleagues (2007) conditionally deleted *Hdac2* in murine cardiomyocytes. Surprisingly, the conditional deletion of the gene in mice hearts (and other tissues like brain, endothelial cells, smooth muscle, and neural crest cells) was as well tolerated as the cardiac conditional deletion of *Hdac1*; a deletion of either of these two in specific tissues displayed no definite phenotypes. As the severe heart defects displayed in the mice suffering from a global deletion of *Hdac2*, could not be observed in the viable animals bearing a cardiac conditional *Hdac2* deletion, Montgomery et al. (2007) consider HDAC2 to play an essential role in various cardiac cell lineages. (Montgomery et al., 2007)

However, if both genes are deleted within the same tissue, serious effects are observable; hence, HDACs 1 and 2 are suggested to operate redundantly during later development of the embryo and throughout the lifetime of the adult organism (Haberland et al., 2008; Montgomery, et al., 2007).

To obtain insight into the in vivo activities of these both enzymes and their redundance capacities, different experiments were performed. A conditional deletion of *Hdac1* and *Hdac2* in cells of the cardiac lineage revealed no obvious phenotype; a single wild-type allele of either of both *Hdac* genes ensures unaffected embryogenesis. On the contrary, a deletion of all *Hdac1* and *Hdac2* alleles causes an escalated expression of genes which encode calcium channels and skeletal muscle-specific contractile proteins in the heart; it is communicate that the up-regulated expression of calcium channel subunit genes

induces a pathological calcium inflow into cardiac myocytes which leads to dysregulated functions of sarcomeres affecting cardiac arrhythmias and dilated cardiomyopathy (represented by an enlarged and weakened heart not able to maintain an efficient ventricular systolic pump function) resulting in neonatal death. (Montgomery et al., 2007) Concerning the severity of the phenotype, the time of deletion was reported to be crucial. In a mouse embryo at developmental stage E8.5 (embryonic day 8.5) a deletion of both *Hdacs 1* and *2*, in the cardiac tissue leads to death 2 days later; if the deletion occurs in the heart of a 10.5 day old embryo, the mouse postnatally lived for more than 3 weeks. Thus, it was suggested that the severity of the phenotype decreases with the progression of development. (Haberland et al., 2008)

Transcriptionally analysing these mice showed that deleting *Hdac1* and *Hdac2* in the heart induces specific gene cascades which exert influence on the Ca^{2+} ion handling and the contractility of cardiac cells; the upregulation through derepression involved 0.94% of transcripts (162 genes) and 0.58% of the transcriptome (100 genes) were down-regulated. Further analysis demonstrated an inappropriate up-regulation of calcium channel subunit genes and skeletal muscle contractile protein genes. (Montgomery et al., 2007) The expression of several calcium channels and skeletal muscle-specific contractile proteins in the embryonic cardiac tissue is transcriptionally regulated by the interaction of neuron-restrictive silencer factor (NRSF) (Kuwahara et al., 2003) with class I HDACs and HDACs 4 and 5 (class IIa HDACs) (Nakagawa et al., 2006). If NRSF is, due to a mutation, incapable of recruiting proteins with repressive deacetylase activity, the transcription of genes anticipating in calcium flux and contractility becomes activated resulting in cardiac defects and lethality as described above (Kuwahara et al., 2003; Montgomery et al., 2007). Consequently, a deletion of *Hdacs 1* and *2* within a cell creates the same effects because NRSF and also other transcription factors fail to form a repressive complex (Haberland et al., 2008). However, Montgomery et al. (2007) imply that the up-regulation relates not only to genes controlled by NRSF; HDACs 1 and 2 are suggested to repress certain genes involved in cardiac contractility by an NRSF-independent mechanism (Montgomery et al., 2007).

After taking all these data into account, HDAC1 and HDAC2 were found to have crucial functions within cardiac development, in which the enzymes seem to work partially redundantly (Brunmeir et al., 2009).

As mentioned in the previous chapter, a conditional delition of *Hdac3* in a mouse heart results in an affecting ligand-induced increase of lipids within the organ ending in lethality after 3-4 month after birth; examining the heart at this point of time, a severe

hypertrophy with enlarged right and left atria was observable. In the heart the gene programs regulating fatty-acid intake and metabolism are influenced by a nuclear receptor protein called peroxisome proliferator-activated receptor alpha (PPARα) which acts as a transcription factor controlling gene expression. The absence of the repressive HDAC3 causes a steep rise of PPARα activity being responsible for the subsequent metabolic disturbance. (Montgomery et al., 2008)

Moreover, deletion of *Hdac3* in the heart shows another phenotype; an escalated generation of collagen due to fibroblast proliferation leads to cardiac dysfunction (interstitial fibrosis) being phenotypically not dependent on increased action of PPARα. However, up to now it cannot be taken for granted that HDAC3 operates as a direct repressor of the transcription factors controlling the fibrotic gene cascade. (Montgomery et al., 2008)

If *Hdac3* is not deleted but over-expressed in the heart, the proliferation of cardiomyocytes increases without expansion of cell size (hyperplasia) causing enhanced thickness of the myocardium (Trivedi et al., 2008).

Concerning the expression of *Hdac8* in the heart, there exist opposing results. Buggy et al. (2000), Hu et al. (2000), and Van den Wyngaert et al. (2000), independently trying to detect *Hdac8* expression sites, found low levels of *Hdac8* mRNA in human cardiac tissue, whereas a more recent study reports about an exclusive *Hdac8* expression in smooth muscle cells; no *Hdac8* transcripts were observed in the heart (Waltregny et al., 2004). However, Wilson and colleagues (2010) demonstrated that in mice HDAC8 and sirtuin 1 homolog (Sirt1; which is also a deacetylase) interact independently with the estrogen-related receptor α (ERRα) in vivo; the enzymes enhance the transcriptional function of ERRα. The elimination of HDAC8 and Sirt1 reduces the affinity of ERRα to bind to the DNA. (Wilson et al., 2010) The ERRα belongs to the nuclear receptor superfamily regulating various target genes which encode for enzymes being involved in the maintenance of energy balance in animals; ERRα is one of the important regulators of endogenous lipid metabolism. In mice ERRα was found to be expressed at a high level in cardiac tissue (Ranhotra, 2009; Stein & McDonnell, 2006) because the heart prefers fatty acids as substrate for cellular energy production (Ranhotra, 2009). Hence, it may be possible that HDAC8 plays an indirect role in the energy metabolism of the heart via transcriptional regulation of ERRα; if *Hdac8* is expressed in the mammalian heart remains to be fully elucidated.

1.3. Class I HDAC expression patterns during mouse and chick development

Up to now several studies about in vivo functions of HDACs exist in mice; in other model systems results are rare. For that reason, I want to compare the expression sites of chicken embryos to that of mice during development, so that similarities and differences could be recognized more easily.

A recent study of class I HDACs in chicken embryos provides new knowledge about the spatio-temporal expression pattern of HDACs 1, 2, 3 and 8 during the avian development. Additionally, the observations were compared to the quite different expression profile during mouse embryogenesis.

Sequencing the chicken (Gallus gallus) genome demonstrated that it includes four genes being highly related to the mouse and human class I HDACs: *Hdac1*, *Hdac2*, *Hdac3*, and *Hdac8*.

The homologies of class I HDACs full length protein sequences between chicken and its mouse equivalents were found to be even higher than the similarities of class I HDACs within the same species. (Murko et al., 2010)

The expression of class I HDACs is considered to be omnipresent during embryogenesis. However, a recent review imparted fluctuating mRNA and protein levels between developmental stages and between species (Brunmeir et al., 2009; Murko et al., 2010).

1.3.1. Expression levels during development

Using qPCR, in chick embryos, *Hdacs* 1, 2, 3, and *8* were found to be expressed in a similar temporal pattern during the early stages of development (HH2-HH17). All class I HDACs showed highest expression levels during early gastrulation (HH2-3 correspond to 6-13 hrs.), a subsequently weakening signal until reaching the lowest quantity at HH8-HH11 (stages of neurulation; correspond to ~1.1-1.9 days), followed by another rise of protein expression. (Murko et al., 2010) Ma and Schultz (2008) gained similar results having performed experimentation in mouse preimplantation embryos; the embryos exhibited high expression levels of most class I HDACs at the blastocyste stage (Ma & Schultz, 2008).

Hdacs 1 and *2* display high expression levels in mouse and can be detected throughout all prenatal developmental stages until birth and even in adulthood. *Hdac2* mRNA is already observable in the fertilized oocyte and also HDAC1 protein can be identified in the nuclei of a two-cell stage embryo, in which the zygotic genes become just activated.

A maximum of *Hdac1* expression was detected during gastrulation of the mouse embryo. (Brunmeir et al., 2009)

In contrast, Zeng et al. (2004) were not able to observe a conclusive signal for HDAC8 in the preimplantation stages of mouse embryos (Zeng et al., 2004). However, during chicken embryogenesis Murko et al. (2010) already detected *Hdac8* transcripts at the earliest developmental stage examined which was ~6-7 hours after incubation (HH2). (Murko et al., 2010)

During later developmental stages Western Blot Analysis gave insight of class I HDAC expression levels throughout the embryo. For having the opportunity to compare chick and mouse development, corresponding stages of the embryogenesis of the two model organisms were observed: Chick HH13 (2-2.2 days) corresponds with mouse E10, chick HH17 (2.2-2.7 days) matches mouse E11.5 and HH25 (4.5 days) in chicken development is like E13 in mouse embryogenesis.

In chicken *Hdac1* levels of transcripts are low at developmental stages HH13 and HH17, subsequently intensifying at stage HH25. In contrast, during mouse embryogenesis a high degree of expression is already observed at stage E10 ensued by diminished levels at stages E11.5 and E13. *Hdacs 2* and *3* display similar patterns during chick and mouse development with a nearly consistent expression level throughout the different embryonic stages. *Hdac8*, like *Hdac1*, shows contrasting trends on protein levels for chicken and mouse embryogenesis. Whereas the chicken embryo demonstrated a heightening accumulation of *Hdac8* transcripts towards stage HH25, in the mouse embryo highest levels of protein expression were detected at stage E11.5 followed by a fast decline to a quantity barely perceptible at stage E13. (Murko et al., 2010)

1.3.2. Spatio-temporal expression patterns

All class I HDACs show overlapping expression patterns in chicken and mouse embryos. However, due to some species specific characteristics observed, individual roles of HDACs in embryogenesis must be taken into account.

In both model organisms, mouse and chick, *Hdacs 1, 2, 3*, and *8* display a high level of expression in the brain vesicles, presenting a higher accumulation of transcripts in the prosencephalic areas and decreasing expression towards the rhombencephalic regions.

In chicken embryos at developmental stage 12 according to Hamburger and Hamilton (1951) (HH 12) class I HDACs are expressed at sites of anterior and posterior neural tube closure; especially HDAC1 is detected. Moreover, during chick embryogenesis class I

HDACs seem to anticipate in the development of the neural crest, in parts of the sensory and the musculo-skeletal system, several internal organs and the branchial arches, which themselves hold a panoply of developmental capacities. These results were gained through whole mount in-situ hybridization (WMISH) by Murko and colleagues (Murko et al., 2010).

Histone deacetylase 1

During chicken development HDAC1 is first recognized as a faint signal in all three primary brain vesicles and the developing neural tube at stage HH10. Between HH10 and HH13 a prominent expression in the brain and the open posterior part of neural tube, which is just about to close, is detected. After neural tube closure, the *Hdac1* protein level diminishes vigorously. Murko et al. (2010) suggest an important role of HDAC1 in neural tube closure. This thesis is supported by preliminary data, showing that a knock down of the enzyme at the expression hot spot results in neural tube closure defects.

As development proceeds, the overall expression of *Hdac1* is maintained, however, at a decreased level at stage HH17. This state of low transcript level is changed at HH25 with pronounced positive labelling in the face mesenchyme, the otic vesicles, and the wing and limb buds.

The internal organs were the last to present *Hdac1* expression. In the lung and liver anlagen low intensities of the enzyme were observable at stages HH17 and HH18; at stage HH25 (~4.5 days) the heart was found to show slight expression as well. (Murko et al., 2010)

From embryonic day E10 to E13 the mouse embryo shows a similar spatial expression pattern of *Hdac1* as the ortholog in the avian model system at stages HH10 and HH13; an expression signal is detected in the brain and in the caudal part of the neural tube being subjected to neural tube closure. A high expression of the enzyme is also observable in the otic vesicles, in the 4 developing limbs and in the branchial arches. Relating to the neural tube, Hdac1 expression was discovered to be restricted to the inner ependymal layer determined to become certain epithelial cells lining the cerebrospinal fluid-filled brain ventricles and the central canal of the spinal cord.

In the internal organs, there was only found a weak positive labelling of the liver anlage at E11.5 and at E13 the genital tubercle showed expression of *Hdac1*. (Murko et al., 2010)

Histone deacetylase 2

Hdac2 expression in chick is first observable at HH12 in the forebrain and in otic and optic vesicles. At developmental stage HH14 the brain and the developing sensory organs remain positively stained; furthermore, the head mesenchyme, the first branchial arch, the notochord and growth zones like somites and the tail bud display *Hdac2* expression. The prominent positive labelling of the brain and head area and the otic and optic vesicles is sustained from stages HH18 to HH24; at stage HH19 a high expression level is also perceptible in all branchial arches, the neural crest cells, the wing and limb buds.

In the internal organs the first expression of *Hdac2* is observed in the nephric ducts at stage HH12 and remains at HH14 and HH15. Further on, at about day 4 of embryogenesis, a high expression rate of the enzyme is observed in the lung buds. No perceptive signal of HDAC2 was found in the developing heart of the chick.

In the mouse embryo *Hdac2* expression is detected in the brain and spinal cord at all developmental stages observed (E10 to E13). Concerning the neural tube, transcripts of *Hdac2* are exclusively found in the middle cell layer, also called mantle layer which is destined to generate the gray matter of the CNS. Compared to the expression site of Hdac1 within the neural tube, the expression domains of both enzymes in the spinal cord are obviously spatially separated; the suggestion of functional redundancy is questioned. However, in the chicken embryo *Hdacs 1* and *2* revealed an overlapping expression pattern in the spinal cord, where the enzymes are accumulated at low levels at developmental stage HH25 (the equivalent of E13 in mouse embryogenesis). Possibly, the spatial separation of HDAC1 and HDAC2 manifests in a later embryonic stage of chicken development. (Murko et al., 2010)

Furthermore, the limb buds show high *Hdac2* expression from E10 to E13. At E11.5 the positive labelling expands to the olfactory placodes and the vibrissae anlage; in the latter the enzyme is still found at E13. The branchial arches and their derivates, respectively, evince the hybridization signal throughout the investigated developmental stages.

The only internal organs being positive for *Hdac2* transcripts are the genital tubercle and the developing liver, both displaying the expression of the enzyme at stage E11.5. (Murko et al., 2010)

Histone deacetylase 3

In the embryonic organism of the chick HDAC3 is first recognizable at HH14 and HH15 in the brain vesicles, neural tube and notochord; the signal expands to the head mesenchyme at HH18 and keeps its spatial expression pattern in the CNS and head region at HH24. The optic vesicles, the limb buds and the branchial arches show a high *Hdac3* expression rate at HH18; at HH24 the strong positive labelling extends to the somites. In the developing internal organs, like liver, lung, and heart, the expression signal is detected at stage HH24.

At developmental day E10 in the mouse HDAC3 was located in the brain where the protein is restricted to areas of the fore and midbrain. In addition, the enzyme is also clearly observable in the otic vesicles at E10. The limb buds and face mesenchyme of the mouse embryo displays an only low expression level of *Hdac3* at E11.5 and E13. Moreover, at E11.5 *Hdac3* was expressed in the genital tubercle; the signal intensifies at E13, at which a low expression rate of *Hdac3* was observed in the embryonic liver as well.

Generally, *Hdac3* presents a comparable spatial and temporal expression pattern as *Hdacs 1* and *2*; however, for the enzyme's anticipation in quite distinct repressive complexes, HDAC3 suggests to have different biological capacities than the other class I HDACs. (Murko et al., 2010)

Histone deacetylase 8

During chick development *Hdac8* expression is evident in all regions of the developing brain, continuing in the neural tube, in the notochord and head mesenchyme at stages HH9 to HH16, diminishing towards HH23. Between HH16 and HH23 the enzyme expands throughout the organism and becomes also detectable in the optic and otic vesicles and nose placodes, the tail and limb buds, the branchial arches; a low degree of expression is observable in the developing nephric ducts, lung buds, liver, and heart anlagen.

In the mouse embryo a modest or low signal intensity of *Hdac8* is found to be strictly confined to the pros- and mesencephalic areas of the vertebrate brain at stages E10 and E11.5. At stage E13 a severe decrease of expression was noticed; HDAC8 is almost imperceptible. (Murko et al., 2010)

Lein et al. (2007) performed in situ hybridization experiments exhibiting a ubiquitous signal of *Hdac8* expression in the brains of adult mice with highest levels of transcripts in parts of the fore and hindbrain (Lein et al., 2007).

On the contrary, another study communicated the total absence of HDAC8 expression throughout the human nervous system enclosing the brain and spinal cord. The experimentation revealed an exclusive *Hdac8* expression in human cells determined to differentiate into smooth muscle. (Waltregny et al., 2004)

Otherwise, as mentioned in a previous chapter, a global deletion of *Hdac8* in mice was found to cause skull instability due to a highly specific inadequacy of cranial neural crest cells (Haberland et al., 2009).

The original papers attempting to determine *Hdac8* expression sites report that *Hdac8* mRNA was found in various human tissues (Buggy et al., 2000; Hu et al., 2000; Van den Wyngaert et al., 2000).

In short, approaches of explanation for these seemingly conflicting results throughout different species remain to be elucidated (Murko et al., 2010).

1.3.3. Class I HDAC expression in the heart

In this chapter I want to summarize the expression profiles of class I HDACs in the heart of chicken and mouse embryos. Concerning the hearts of mouse embryos, the whole mount in-situ hybridization brought no conclusive results. Although there exist studies in mice inquiring cardiac specific class I HDAC knock-outs and their consequences (presented in the previous chapter), Murko et al. (2010) found no detectable hybridization signals of HDACs 1, 2, 3 and 8 in the embryonic mouse heart which is possibly due to species specific technical limitations of the WMISH.

In chicken hearts Murko et al. (2010) detected low hybridization signals for HDAC1 at developmental stage HH25 (~4.5 days) and for HDAC8 between HH16 (~2.1-2.3 days) and HH23 (~3.5-4.0 days). A moderate level of *Hdac3* expression was observable at stage HH24 (~4.0 days); earlier observations of *Hdac3* in the embryonic heart revealed a low expression rate of the enzyme already present at stage HH18 (~2.7-2.9 days) (Murko et al., unpublished data). For HDAC2 no perceptive positive labelling was found in the developing heart of the chick (Murko et al., 2010).

At the time of the first detection of class I HDAC expression in the heart of the chicken embryo, the cardiac development has already undergone several crucial processes: By now the heart consists of 3 layers, the endocardium, the myocardium, and the

epicardium and lies within the pericardial cavity. The looping of the simple heart tube has begun previously and is about to be finished at stage HH16, when expression of class I HDACs is firstly localized in cardiac tissues. At that time, cells from the secondary heart field, derived from splanchnic mesoderm, have started to become incorporated into the myocardium of the ventricular outflow tract. At about HH14 the septa of the heart have begun to form. The interatrial septum, dividing the early single atrium in a left and a right cavity, is the first visible septum, arising as a ridge at the cranial dorsal wall of the single atrium. At HH16 the atrio-ventricular cushions, building the future septum between the atria and ventricles, are established of the dorsal and the ventral wall of the heart; at about HH24 the cushions meet in the midline and fuse. At the same developmental stage the interatrial septum starts to connect with the cushions. The division of the originally single ventricle into 2 separated chambers becomes induced at HH20-24 when the left and right portions of the primary ventricle bulge; the remaining part of the initial wall of the single ventricle is the basis of the interventricular septum. This septum originates at the apex of the heart and grows towards the atrio-ventricular cushions; with these the septum coalesces at about stage HH29. Right after the bulging of the ventricles, at HH24-27, far-ranging trabeculae carnae become generated at the ventricular walls and cause these to thicken intensely and to grow muscular. At stage HH27 the left and right atria become muscular as well; subsequently, at HH31-37, these newly established bands of muscle form so called “muscular arches” which are unique for avian atria. Furthermore the cardiac valves (venous, sinu-atrial, and atrio-ventricular valves) generally begin to develop at HH24-27. The aortico-pulmonary septum, essentially derived from neural crest cells which previously have migrated into the developing outflow tract, branches the truncus arteriosus into the aorta and the pulmonary artery. This process becomes initiated at about HH27 and is characterized by considerable apoptosis and remodelling to enable convenient positioning of the great vessels over their corresponding/proper ventricles; consequently, at HH31 the left ventricle has gained direct access into the aorta and the right ventricle joins the pulmonary artery. (Bellairs & Osmond, 2005)

Which role do class I HDACs play in the cardiac development of chicken embryos? Do they hold essential functions in the developmental processes of the heart or do they only take a marginal part?

2. Methods and Material

2.1. Exposure of the embryonic heart to the histone deacetylase inhibitor in ovo

2.1.1. The choice of the HDAC inhibitor and its carrier

Trichostatin A (TSA)

Trichostatin A (TSA) is an organic product of Streptomyces sp. used as a standard HDAC inhibitor whose effects are reversible. TSA is a so called pan-HDAC inhibitor targeting several classic HDAC isoforms; TSA inhibits the action of all mammalian HDAC members of class I and II (HDACs 1-10). (Zhao et al., 2009)

TSA reversibly blocks the elimination of acetyl moieties from the lysine residues of core histones performed by HDACs (Taunton, Hassig, & Schreiber, 1996); consequently, TSA escalates the level of histone acetylation (Zhao et al., 2009) and influences the access of transcription factors and complexes to genes (Taunton, Hassig, & Schreiber, 1996). This elevation of acetylated histones seems to be dose-dependent: Mouse mammary gland tumor cells (FM3A) being exposed to 6.7nM TSA showed accumulation of di- and tri-acetylated histone H4 coinciding with a decrease of non-acetylated H4; an increase of tri- and tetra-acetylated H4 and acetylation of alternative core histones were more significant in cells treated with TSA concentrations higher than 33nM. Thus, the effect of TSA is noteable at low concentrations in the nanomolar range. (Yoshida et al., 1990)

The inhibition of histone deacetylation by TSA is assumed to cause derepression of silenced genes in multicellular eukaryotic organisms (Zhao et al., 2009). In Xenopus laevis embryos having been exposed to 30nM TSA were also found to promote histone hyperacetylation; no interference with cell division or differentiation being important for appropriate morphogenic development was observable (Almouzni et al., 1994). Additionally, in pregnant mice having received an injection of 15 µg of TSA (dissolved in 0.2 ml of Dimethylsulfoxide DMSO) into the abdominal cavity, neither apparent effects of toxicity for the mother or for the developing embryo nor teratogenicity were recognized; the only detectable consequence of the in vivo TSA administration was the disturbed mammalian embryogenesis due to the altered gene transcription caused by TSA induced HDAC inhibition (Nervi et al., 2001). Furthermore, two different concentrations of TSA were tested on avian limb buds to determine the effects of TSA on apoptosis and gene expression in the model system “chicken”. 750 µM or 75µM of TSA were loaded on acrylamide beads which were implanted in the developing limbs; the beads with the higher loading released about 310.0 to 320.0 nmol TSA per µg beads

and the beads soaked in 75µM TSA set 23.5 to 25.0 nmol TSA per µg beads free. It was shown that the concentration of 750 µM TSA causes cell death and abberations in limb development; the latter are possible secondary effects on gene expression originating from apoptosis. Moreover, 12 hours after TSA application on the limb buds apoptosis was more pronounced than after 24 hours. Lower concentrations of 75µM TSA did not result in cell death, hence, the detected alterations in embryonic development establish unassociated to apoptosis. (Zhao et al., 2009) Besides apoptosis, in cancer cells (Chiba et al., 2004; Hoshikawa et al., 1994; Yoshida et al., 1990) as well as in rat fibroblast cells (Yoshida & Beppu, 1988), a disturbed cell cycle and differentiation are consequences of the cells' treatment with TSA. TSA blocks the G1 and/ or G2/M phases of the cell cycle; consequently, the cell growth is inhibited. (Chiba et al., 2004; Hoshikawa et al., 1994; Yoshida & Beppu, 1988) Chiba et al. (2004) suggest that the suppression of the growth phases depends on TSA concentration and on the point of time it is applied to the cells (Chiba et al., 2004).

In summary, Trichostatin A is a potent HDAC inhibitor which in general is well tolerated in vivo and whose efficacy is mostly dose-dependent. Its good in vivo compatibility is attributed to the inhibitor's incomplete prevention of HDAC activity (in comparison to a genetic deletion which results in a total lack of an HDAC) and its only temporary effects. In addition, TSA is considered to inhibit only the enzymatic activity without interfering with the repressive complex. (Haberland et al., 2008)

Dimethylsulfoxide (DMSO)

Dimethylsulfoxide (DMSO) is a low-molecular weight compound used as a main organic (co-)solvent which increases the solubility of substances to perform experiments involving the necessity of cell permeation (Da Violante et al., 2002). DMSO facilitates the transport of several substrates across cell membranes (Penninckx et al., 1983); hence, DMSO is taken as a vehicle for TSA (Nervi et al., 2001). DMSO is soluble in organic and in aqueous media, therefore, it finds use in solubilizing insufficiently soluble compounds. For being a carrier substance, DMSO is also used as a solvent for poorly water-soluble drugs which need to be absorbed by the skin (e. g. insulin and sulfadiazine). (Da Violante et al., 2002) A further characteristic of DMSO is its protection of cell membranes against the effects of freezing (Penninckx et al., 1983); accordingly, the solvent is a valuable cryoprotectant (Da Violante et al., 2002; Penninckx et al., 1983). Besides these beneficial qualities, DMSO has some detrimental toxic effects; the solvent is described to affect the

cell membrane and the cell metabolism causing severe damaging of the cell inducing apoptosis. (Da Violante et al., 2002)

Penninckx and colleagues (1983) performed experiments aiming to determine the consequences of various DMSO concentrations on dog kidney tissue under different conditions. They reported that DMSO concentrations exceeding 10% induced disturbance of the membrane integrity and the metabolism of the cell. Morphologically the toxicity of DMSO levels higher than 10% resulted in autolytic lesions such as degeneration of the cell nucleus, vacuolization of the renal epithelial tissue, and separation of the basement membrane (lying under the epithelium) of the kidney; these effects were observed at room temperature after 60 minutes of DMSO incubation. If the temperature is escalated to 37°C and/ or the exposure time is extended to 120 minutes, the cell/ tissue damage becomes more severe. (Penninckx et al., 1983) Concerning the temperature Malinin et al. (1967) witnessed the same result in HeLa cells (human epitheloid cervical carcinoma cell line): The degree of cell viability decreases with rising temperature while maintaining the concentration of DMSO unchanged. (Malinin et al., 1967)

Da Violante et al. (2002) also tested the effects of different concentrations of DMSO on cell monolayers of the human colon tumor cell line Caco2 clone TC7 (Caco2/ TC7) at 37°C; the cells were exposed to DMSO for 120 minutes. Up to a concentration of 10% DMSO the viability of the cells remained unchanged; when higher concentrations were administered to the cells, a drastic decline of viable cells was observable. At a DMSO concentration of 20% the percentage of viable Caco2 cells was reduced from 100% (negative control) to 73%. Besides the maintained cell viability, at 10% DMSO no manifested cytotoxicity could be examined; in contrast to higher concentrations the permeability of the apical membrane and the cell-to-cell tight junctions remained unaffected at DMSO 10%. (Da Violante et al., 2002)

Previous studies demonstrated that the cell type is a further crucial factor for the cells' viability. Branch and colleagues (1994) performed experiments with human bone marrow hematopoietic progenitor cells to investigate the suggested toxicity of DMSO to these types of cells. They found out that particularly colony-forming units granulocyte/macrophage (CFU-GM) remain undisturbed after exposure to 8.5% DMSO for 120 minutes, whereas the viability of some mononuclear cells became diminished under the same conditions. (Branch et al., 1994) Malinin et al. (1967) showed that HeLa cells display alterations after being exposed to DMSO concentrations higher than 5-10%; the changes examined were independent of the length of exposure (Malinin et al.,

1967). Watanabe et al. (2000) reported that a concentration of 5% DMSO did not result in damage of the cell membranes of isolated rat intestinal tissue in permeation studies using an Ussing chamber (scientific equipment used to determine ion transport in tissues); the experiments took up to 100 minutes (Watanabe et al., 2000). Nervi et al. (2001), already mentioned in the previous chapter for using pregnant mice for their experiments with TSA, injected 0.2 ml of DMSO into the mice' abdominal cavity to use them as controls for the TSA treated mice; they could not observe any apparent alterations in the embryo or the mother (Nervi et al., 2001).

Taking these various factors influencing toxicity (concentration, exposure time, temperature, and cell type) into account, Dimethylsulfoxide is a sufficient carrier substance in multiple experimentations.

2.1.2. Preparation of TSA for administration to the embryonic hearts

TSA was applied to heparin-acrylic beads (0.57 mg heparin/ml packed acrylamide gel; Sigma, H5263). All centrifugation steps were carried out in a mini-centrifuge (Sprout) at maximum speed (6000 rpm). The used Locke-solution (isotonic electrolyte-containing solution used to keep living samples for experimental purposes) was autoclaved.

500 µl of the beads in saline suspension were centrifuged for a few seconds and the supernatant was discarded. 500 µl of Locke-solution were added to the beads, and after vortexing for about 30 sec, the beads were centrifuged again. This step was repeated twice. Before the last centrifugation step, the beads were divided equally into two 500-µl-Eppendorf tubes; to one half of the beads TSA was added and the other half was soaked in DMSO for control embryos. After centrifuging, the supernatant was removed, so that 100 µl of the beads in Locke-solution remained in each tube. Subsequently the beads were incubated with 5 µl of TSA stock solution (1 mg/ml) or 5 µl DMSO 1%; the final TSA concentration was 165.36 µM and the concentration of DMSO was 0.05%. Both tubes were vortexed and kept at 4°C overnight (o. n.) in a horizontal position. On the next day the tubes were centrifuged and the supernatant discarded. The following washing step was repeated twice: 400 µl of Locke-solution were added to the beads; after vortexing and centrifuging, the supernatant was removed. Again 400 µl of Locke-solution were transferred to the beads; the tubes were vortexed and kept at 4°C for 1 h. The subsequent wash of the beads was accomplished by vortexing and centrifuging the tubes and removing the supernatant. This washing step was repeated using 200 µl of Locke-solution; the remaining supernatant covered the beads to avoid dehydration. At last, the tubes were put on ice; the beads were ready for use. (Zhao et al., 2009)

Besides the implantation of beads, 2 different concentrations of TSA were tested for direct injection into the pericardial cavity of the embryonic heart. The desired TSA or DMSO concentrations were achieved by dilution of TSA stock solution (1 mg/ml) or pure DMSO with Locke-solution; the final concentrations were as follows: 165.36 µM TSA and 0.05% DMSO; 50 µM TSA and 0.015% DMSO. TSA and DMSO solutions were labeled with vital dye fast green (Sigma-Aldrich) to be able to locate the exact injection site, i.e. the pericardial cavity. Fast green was prepared as a 1% solution (the dye was dissolved in Aqua dest.); the dye solution was used 1:10 to the final volume of TSA or DMSO solutions.

Locke-solution, pH 7.4
8.5 g NaCl
0.42 g KCl
0.24 g $CaCl_2$
1000 ml Aqua dest.

DMSO 1%
Pure DMSO
Locke-solution

TSA stock solution (1 mg/ml)
1 mg TSA
1 ml DMSO 1%

2.1.3. Exposure of the embryonic hearts to TSA in ovo

Fertilized chicken eggs (White Leghorn, Gallus gallus domesticus) were acquired from a breeder in Gloggnitz, Lower Austria (Schropper). The eggs were incubated at a temperature of 37°C and relative humidity of 60% for 4 days up to Hamburger-Hamilton (HH) stages 23-24. The determination of the developmental stages of the chicken embryos accords to Hamburger, V. and Hamilton, H. L. (1951). The embryo exposure to TSA in ovo was performed with sterile surgical instruments.

Prior to aspirating 1.5-2.0 ml of egg white through the air sac, the egg shell atop of the air sac was incised with a fine saw to facilitate the access with the syringe. The eggs were windowed using a fine saw and forceps. Afterwards the embryos were hoisted by compensating the reduction of egg white with Locke-solution (used as an egg white substitute) to support the following operation steps taking place under a stereo microscope (Leica IC80 HD): Within the operation field the vitelline membrane, the inner

and outer membrane of the amniotic sac, the ectoderm and the pericardium were cut open with a tungsten needle. For better differentiation of the membranes Nile blue sulfate (0.1 mg/ml PO_4 buffer) was used to stain them. The beads having been soaked with TSA or DMSO (for the control embryos) were absorbed up a pulled glass needle attached to a rubber tube and positioned near the embryo. With a blunt needle 1-4 beads were pushed through the slit in the pericardium (which should not be to long so that the beads stay at the desired position) and remain in the pericardial cavity of the embryo.

As mentioned in the previous chapter, 2 different concentrations of TSA and DMSO were tested by direct injection. Like the beads, the injection solutions were soaked up a fine pulled glass needle attached to a rubber tube and directly injected into the pericardial cavity of the embryonic heart.

After the implantation of the beads or the injections, the embryo was once again lowered by aspiration of the egg white with a syringe. The operation window and incised air sac were sealed with medical tape. Subsequently, the eggs containing embryos with implanted beads were reincubated for 36-48 h; the embryos having been injected were reincubated for 8-24 h.

2.1.4. Removal and fixation of the treated embryonic hearts

The operation window of the reincubated eggs was reopened, the developmental stages of the embryos were determined in accordance to Hamburger and Hamilton and deviations were documented. Next, the embryo was cut out of the egg, put into a Petri dish filled with Locke-solution and freed from the enclosing membranes. The embryonic heart was removed by using appropriate surgical instruments and again aberrations were noted. Immediately the heart was photographed under a microscope (Leica MZ16 F) equipped with a digital camera (Nikon DN100). Next, the heart was fixed in 4% PFA for 24 h; subsequently, PFA was replaced by 1x PBS.

<u>1x PBS, pH 7.4</u>
150 mM NaCl
16.69 mM Na_2HPO_4
1.66 mM NaH_2PO_4
Aqua dest.

PFA 4%, pH 7.4
1x PBS
4% PFA

2.2. Histological and morphometric analysis of the treated embryonic hearts

2.2.1. Paraffin embedding and sectioning

After fixation with PFA 4%, the hearts were washed 3 times for 30 min with 1x PBS. The specimens were dehydrated by incubation in a graded ethanol series beginning with the lowest and ending with the highest concentration; ethanol concentrations were as follows: 60% - 70% - 80% - 90% - 95% - 100%. In each of the different concentrations the samples were kept for 30 min; 100% ethanol was administered twice to the hearts, each time for 30 min. Subsequently, methyl benzoate was added to the hearts for 4 times; each time the hearts had to sink to the bottom of the vial before the methyl benzoate was changed. Afterwards the methyl benzoate was replaced by benzene for 2.5 min. After repeating the benzene step 3 times, a mixture of benzene and soft paraffin was applied to the samples for 5 min. All these steps were carried out with tightly capped vials to prevent evaporation of the alcohol; the following procedures were performed with uncapped vials. Next, the benzene-soft paraffin mixture was removed and pure soft paraffin was added to the hearts; the vials were incubated for 30 min at 40°C. Afterwards, 4 paraplast changes were accomplished: The first change took place after incubation for 30 min, 1-2 h later the next paraplast change was performed and the last 2 incubations with paraplast took 3-4 h each. After each exchange the vials were put into the incubator at 60°C. The incubation of the samples in 70% ethanol, the methyl benzoate step, and the last 2 paraplast changes could be accomplished o. n.. The described procedures were applied to the hearts with implanted beads. The numerous specimens obtained by injection experiments were embedded by an automatic embedding machine (medite Tissue Processor TPC 15). The first steps of paraffin embedding (till the incubation of the hearts in 70% ethanol) were carried out manually; afterwards the embedding machine was programmed as follows:

Step	Incubation in …	Temperature	Time (h:min)
01	Ethanol 70%	30°C	1:00
02	Ethanol 70%	30°C	1:30
03	Ethanol 80%	30°C	1:00

04	Ethanol 80%	30°C	1:30
05	Ethanol 96%	30°C	1:00
06	Ethanol 96%	30°C	1:30
07	Ethanol 96%	30°C	2:00
08	Xylene	30°C	0:30
09	Xylene	30°C	1:00
10	Xylene	30°C	1:30
11	Paraplast (melting point at 60°C)	55°C	1:30
12	Paraplast (melting point at 60°C)	55°C	1:30
13	Paraplast (melting point at 60°C)	56°C	2:00
14	Paraplast (melting point at 60°C)	56°C	2:30

The ensuing embedding of the hearts took place at an embedding station: An embedding boat was half filled with paraplast and the heart was properly positioned for sectioning with pre-heated forceps. The embedding boat was shortly put on the freezing plate of the embedding station; thus, the paraplast began to solidify at the bottom of the boat and the position of the sample was fixed. An embedding cassette without lid was placed above the sample in the embedding boat which then was filled up with paraplast. Subsequently, the embedding boat was deposited on the freezing plate for about 1 h till the paraplast had solidified completely.

Afterwards the solid paraplast block with the embedded sample was trimmed and sectioned at a thickness of 4 µm using a microtom (Thermo Shandon Finesse); the hearts were sectioned serially. The longitudinal sections were mounted onto HistoBond adhesive slides (Marienfeld) and incubated o. n. at 42°C to bind the sections to the slides.

2.2.2. Mayer's hematoxylin and eosin staining

The HistoBond adhesive slides were sorted into a cuvette. Before the staining procedure began, the sections were deparaffinized and rehydrated. For deparaffinization the slides were put in xylene 3 times, each time for 7 min. The following rehydration occurred by incubation of the slides in a graded ethanol series beginning with the highest and ending with the lowest concentration; ethanol concentrations were as follows: 100% - 95% - 90% - 80% - 70% - 60%. In each of the different concentrations the samples were kept for 3 min; 100% ethanol was administered twice to the slides (1 brief wash to remove

the xylene, 1 x 3 min). After rehydration the slides were rinsed twice in distilled water. The staining step followed: Mayer's Hematoxylin (AppliChem, A4840) was filtered and applied to the slides for 2 min. Immediately, the slides were rinsed 3 times in distilled water. The staining was examined under the microscope; if not only the nuclei were stained but also the cytoplasm, a differentiation step followed. The slides were differentiated in 70% hydrochloric acid-ethanol for 6 sec. Afterwards the slides were immediately rinsed twice in distilled water. If necessary the differentiation step was repeated; incubation time was adapted. Subsequently the slides were washed under running tab water for 10 min until the pink stained cell nuclei of the heart sections changed to blue. The slides were rinsed twice with distilled water. Next, the slides were counterstained in filtered 0.1% eosin solution for 2 min (staining the cytoplasm pink) and afterwards rinsed twice with distilled water. Subsequently, the sections were again dehydrated: in 95% ethanol the slides were washed briefly; 2 changes of 100% ethanol followed, 30 sec each. Then the slides were cleared in 4 changes of xylene (1 brief wash, 3 x 3 min). At last the sections were mounted with Eukitt Mounting Medium (xylene based synthetic resin).

Eosin stock solution 1%
1 g eosin
Aqua dest. to a final volume of 100 ml

Eosin working solution 0.1%
10 ml eosin stock solution 1%
90 ml Aqua dest. to a final volume of 100 ml
3 drops glacial acetic acid (concentrated, H_2O-free)

2.2.3. Morphometric analysis

After approximately 2 days the mounting medium had dried and the histological stained sections of the embryonic chicken hearts could be examined and photographed using a Nikon Eclipse 800 epifluorescence microscope equipped with a digital camera. Next, the images were measured using ImageJ 1.41 bundled with Java 1.6.0_10; the area of the left and right ventricle and of the atria were the evaluated features. The subsequent analysis comprised the determination of the areal sum of both ventricles and of the areal proportion of atria to ventricles and of left ventricle to right ventricle by using Microsoft Office Exel 2007.

2.3. Analysis of proliferation and apoptosis in the treated embryonic hearts

2.3.1. Bromodeoxyuridine (BrdU) cell proliferation assay

BrdU is a synthetic nucleoside substituting thymidine during DNA replication, thus, it becomes incorporated into the newly synthesized DNA of dividing cells. The detection is achieved with a BrdU-specific antibody.

Before being able to perform the proliferation assay, the embryos had to be treated with bromodeoxyuridine (BrdU) in ovo: 1 h before the embryonic hearts were to be removed, the eggs were reopened and 200 µl of 1x PBS containing 10 mM BrdU(Sigma) were dripped on each embryo. The reopened operation window was sealed with medical tape and the eggs were reincubated for 1 h. After the following removal and fixation of the hearts, the samples were embedded in paraffin and sectioned as described above. On each slide 2 sections were mounted; one section was derived from a BrdU treated heart and the other one was acquired from an untreated specimen (for the negative control). Both sections underwent the same procedures as described below.

The sections were additionally dried at 58°C for 60 min, deparaffinized and rehydrated. For deparaffinization the slides were put in xylene 4 times (3 x 30 min, 1 x o. n). On the next day rehydration occurred by incubating the slides in a graded ethanol series beginning with the highest and ending with the lowest concentration; ethanol concentrations were as follows: 100% (twice)- 95% - 90% - 80% - 70% ethanol mixed with 0.25% NH_3 - 60%. In each of the different concentrations the samples were kept for 5 min; in the solution of NH_3-ethanol the slides were incubated for 45 min. After rehydration the slides were rinsed in distilled water and, subsequently, in 1x TBS. Afterwards the sections were pre-treated with 1x TBS containing 1% $NaBH_4$ for 40 min, then washed in 1x TBS (one brief wash, 1 x 15 min) and rinsed with distilled water. After the washing step another pre-treatment, DNA denaturation of the cells of the sectioned heart tissue, followed: The slides were incubated in 2N HCl at 37°C (water bath) for 60 min. Next, the acid was neutralized by washing the slides 3 times in 0.1M borate buffer (one brief wash, 2 x 5 min). After 4 additional changes of 1x PBS (one brief wash, 3 x 5 min) the slides were pre-incubated in blocking solution at room temperature (RT) in a wet chamber for 45 min. Subsequently, the slides were incubated with the first antibody α-BrdU (mouse) (IgG; Roche) diluted 1:20 in blocking solution at 4°C in a wet chamber o. n. On the next day the slides were washed 4 times with 1x PBST (each wash took 30 min)

before the secondary Alexa 488-labeled α-mouse antibody (goat) (Southern Biotechnology) diluted 1:1000 in blocking solution was applied to the slides for 60 min at RT in a wet chamber. After 3 washes with 1x PBST (one short wash, 2 x 5 min), the nuclei in the heart tissue were counterstained in a DAPI containing solution (0.1 µg DAPI/ml PBST) for 5 min. Additional 3 washes with 1x PBST were followed by mounting of the slides with Citifluor (a non-fluorescent immersion oil containing an antifading agent; Christine Gröpl). The slides were kept at 4°C until examination and documentation of the fluorescently labeled cell nuclei of the embryonic chicken hearts via fluorescence microscopy (Nikon Eclipse 800 epifluorescence microscope).

1x TBS, pH 7.4
20 mM Tris/HCl, pH 7.4
150 mM NaCl
Aqua dest.

Borate buffer, pH 8.5
0.1 M borax (sodium tetraborate)/H_3BO_3, pH 8.5
Aqua dest.

1x PBST
1x PBS, pH 7.4
0.05% Tween 20

Blocking solution, pH 7.4
1x PBST
1% BSA

2.3.2. Terminal transferase dUTP nick end labeling (TUNEL) cell apoptosis assay

TUNEL is a method which enables the detection of DNA fragments caused by apoptosis. The enzyme terminal transferase identifies the presence of nicks in the DNA and catalyzes the addition of dUTPs. The dUTPs are labeled with a marker which can be detected by an antibody specific for that marker.

For the TUNEL assay the embryos did not have to be pre-treated with a chemical substance; instead the 3 sections which have been mounted on each slide (the sample, a positive and a negative control) had to be treated differently.

The first steps of the TUNEL assay (i. e. the additional drying, the deparaffinization, the rehydration, the washing, and the pre-treatment with 1x TBS containing 1% $NaBH_4$)

were the same as for the BrdU proliferation assay. After the pre-treatment of the slides with 1x TBS containing 1% $NaBH_4$, the slides were washed in 1x TBS (one brief wash, 2 x 5 min). The next step was the DNase digest of the positive controls with a DNase containing buffer at 37°C (incubator) in a wet chamber for 10 min. During that digest the negative controls and the samples were incubated with 1x TBS, also in a wet chamber, to prevent the sections from drying. After a rinse and following 2 washes (5 min each) with 1x PBST, the reaction mix containing terminal transferase and a dNTP nucleotide mix including digoxigenin-lableled dUTP was applied to the samples and the positive controls for 30 min at 37°C (incubator) in a wet chamber; each section was incubated in 5 µl of the reaction mix. The negative controls were incubated with a reaction mix excluding the terminal transferase; the amount of the enzyme was replaced by DEPC-H_2O. The incubation of the negative controls took place under the same conditions as the incubation of the samples and positive controls. After 4 changes of 1x PBST (one brief wash, 3 x 5 min) the slides were pre-incubated in blocking solution for 30 min at RT in a wet chamber. Subsequently, the slides were incubated with a FITC-labeled α-Dig antibody (sheep) (Roche) diluted 1:100 in blocking solution at 4°C in a wet chamber o. n. On the next day the slides were washed 3 times with 1x PBST (1 x 15 min, 2 x 30 min). Afterwards the nuclei in the heart tissue were counterstained in a DAPI containing solution (0.1 µg DAPI/ml PBST) for 5 min. Additional 3 washes with 1x PBST (one brief wash, 2 x 5 min) were followed by mounting of the slides with Citifluor (Christine Gröpl). As the BrdU treated sections, the slides were kept at 4°C until the fluorescently labeled cell nuclei of the embryonic chicken hearts were examined and documented using a fluorescence microscope (Nikon Eclipse 800 epifluorescence microscope) equipped with a digital camera.

<u>DNase buffer for DNase digest</u>
50 mM Tris/HCl, pH 7.5
0.1% BSA
Aqua dest.

<u>DNase containing solution</u>
x ml DNase buffer
3 U DNase/ml buffer (DNase stock: 10 U/µl; Sigma)

Reaction mix containing terminal transferase
20% 5x buffer (Promega)
10% nucleotide mix
0.25 U terminal transferase/µl final volume (terminal transferase stock: 30 U/µl; Promega)
x µl DEPC-H_2O to the desired final volume

Nucleotide mix (all dNTPs purchased from Roche)
5 µl 2.5 mM dATP
5 µl 2.5 mM dCTP
5 µl 2.5 mM dGTP
3.4 µl 2.5 mM dTTP
4 µl 1 mM dUTP-Dig
27.6 µl dH_2O to a final volume of 50 µl

2.4. Analysis of the acetylation level of the treated embryonic hearts

2.4.1. Preparation of the hearts for histone isolation

After exposure of the embryonic hearts to TSA or DMSO, the eggs were reincubated for 6 h or 24 h, respectively. Following the removal of the embryos, they were immediately deposited in 1x PBS containing 10 mM sodium butyrate to maintain the acetylation level of the core histones in the nuclei of the cardiac tissue. Surrounded by the sodium butyrate solution, the hearts were extracted and collected in 500-µl-Eppendorf tubes also filled with sodium butyrate solution. The subsequent brief centrifugation step was carried out in a mini-centrifuge (Sprout) at maximum speed (6000 rpm). After discarding the supernatant, the hearts were shock frozen in liquid nitrogen and either stored at -80°C or instantly used for histone isolation.

2.4.2. Histone isolation

100 µl ice-cold histone lysis buffer were added to the frozen hearts which subsequently were homogenized with a pestle. Then a further 900 µl of ice-cold lysis buffer were added to the homogenisate. After vortexing, the samples were centrifuged at 12 500 rpm for 5 min at 4°C and the supernatant was discarded. A wash with the lysis buffer followed: The cell pellet was resuspended in 1 ml of the ice-cold buffer by vortexing vigorously and again centrifuged at 12 500 rpm for 5 min at 4°C; afterwards the supernatant was removed. This washing step was repeated 3 times and followed by an additional wash with 1 ml histone wash buffer. Subsequently, the cell pellet was resuspended in 100 µl ice-cold H_2O, ultrapure (Sigma) and concentrated H_2SO_4 was

added 1:100 to a final concentration of 0.4 N; by the acidic milieu, the histones were dissolved in the liquid. After vortexing, the samples were incubated on ice for at least 2 h. Next, the samples were centrifuged at 14 000 rpm for 10 min at 4°C and 10x volumes acetone (for histone precipitation) were added to the supernatant, which then contained the histones. After an additional vortexing step, the tubes were incubated at -20°C o. n. On the next day, the samples were again spun down at 14 000 rpm for 15 min at 4°C and the supernatant was removed by decanting. Then, the histone pellet was washed twice with acetone: The pellet was resuspended in 1 ml acetone by vortexing intensely and centrifuged at 14 000 rpm for 5 min at 4°C; afterwards the supernatant was decanted or removed with a pipette (if the pellet did not adhere to the tube). After air drying, the histone pellet was resuspended in 10 mM Tris (pH 6.5); that protein extract was either stored at -80°C or immediately used for further experiments.

Histone lysis buffer, pH 6.5
10 mM Tris
50 mM sodium bisulfite
1% Triton X-100
10 mM $MgCl_2$
10 mM sodium butyrate
8.6% sucrose

Histone wash buffer, pH 7.4
10 mM Tris
13 mM Na_3EDTA

2.4.3. Bradford assay

Bradford reagent (Bio-Rad) was diluted 1:5 with dH_2O and filtered through a 45 µm filter. 1 µl of histone extract was added to 1 ml of diluted Bradford reagent. The absorbance of the samples was measured at a wave length of 595 nm with a Bio-Rad SmartSpec™ Plus Spectrophotometer and the protein concentration was determined according to a standard curve. The determination of the concentrations of the different protein samples was needed to be able to load equal amounts of proteins on the gels for SDS-PAGE.

2.4.4. SDS-polyacrylamide gel electrophoresis (SDS-PAGE)

The extracted histones were separated on 16% polyacrylamide gels which were overlaid with 5% stacking gels. The gels had a thickness of 0.75 mm using the Bio-Rad Mini gel system. The amounts of the different components for 2 mini gels were as follows:

Separating gel: 16%		Stacking gel: 5%	
Solution A	4.8 ml	Solution A	1 ml
Solution B	2.25 ml	Solution C	1.5 ml
Aqua dest.	1.95 ml	Aqua dest.	3.5 ml
10% APS	90 µl	10% APS	60 µl
TEMED	7.5 µl	TEMED	5 µl
Total volume	9 ml	Total volume	6 ml

Solution A: 30% acrylamide, 0.8% bisacrylamide
Solution B: 1.5 M Tris/HCl, pH 8.8; 0.4% SDS
Solution C*:* 0.5 M Tris/HCl, pH 6.8; 0.4% SDS

The components of the separating gel were combined and poured into the previously cleaned gel unit and overlaid with a small quantity of isopropanol to ensure the straightening of the top level of the gel. After the polymerization of the separating gel which took 15 min, the isopropanol was removed completely and the components of the stacking gel, having already been mixed, were poured onto the separating gel. Immediately, the comb was inserted and the stacking gel was allowed to polymerize for at least 15 min. Afterwards, the comb was removed and the slots were rinsed with Aqua dest. After putting the gel into the buffer chamber filled with 1x running buffer, the protein samples were prepared as follows: Equal amounts of proteins from the different histone samples were mixed 1:1 with 2x Laemmli buffer containing 5% β-mercaptoethanol (reducing; Bio-Rad) and denatured at 95°C for 5 min. After storing the samples on ice for a few min, the denatured histone samples were loaded on the gel. The gel was run at 80 V until reaching the separating gel and then shifted to a constant voltage of 90 V until the Bromphenol Blue reached the bottom of the gel. 5 µl of Kaleidoscope Prestained Protein Standard (Bio-Rad) served as size marker.
One of the 2 gels was used for Western blot analysis and one was stained with Coomassie Blue.

1x running buffer, pH 8.3
25 mM Tris
192 mM glycine
0.1% (w/v) SDS

Protein samples
x µl histone extract
y µl 10 mM Tris, pH 6.5
(x+y) µl 2x Laemmli buffer

2x Laemmli buffer
62.5 mM Tris/HCl, pH 6.8
25% glycerol
2% SDS
0.01% Bromphenol Blue
5% β-mercaptoethanol

2.4.5. Coomassie staining and gel drying

After running the gels, one of them was stained with Imperial protein staining solution (Pierce) for 1 h and subsequently washed with distilled water o. n. On the next day the background staining was reduced and the bands were clearly visible. Next, the gel and 2 sheets of cellophane paper were equilibrated in gel drying solution (Invitrogen); the gel was only incubated for 30-60 sec, because the drying solution diminishes the staining and makes the gel brittle. After arranging the gel between the cellophane sheets and fixing that sandwich into the gel drying equipment, the gel was dried for at least 8 h. Then, the gel was cut out of the equipment with a scalpel.

2.4.6. Western blot analysis

Semi dry blotting

The transfer of the separated proteins from the SDS-gel to nitrocellulose membrane (Bio-Rad Trans-Blot®) was performed in a semi-dry blotting unit (Bio-Rad Trans-Blot® SD). Before the assembly of the blotting sandwich, the anode and cathode platform of the blotting unit were moistened with 1x blotting buffer. Next, the blot was prepared as follows: First 1 sheet of extra thick filter paper was applied to the blotting unit, followed by the nitrocellulose membrane, the gel, and finally 1 more sheet of filter paper; all components of the blotting sandwich were soaked in 1x blotting buffer before the assembly. To exclude air bubbles within the blotting sandwich, a falcon tube was rolled

over it. The blot was covered with the cathode platform and subsequently with the lid of the blotting unit. The protein transfer was performed for 30 min at 20 V. To check the efficiency of the blotting, the membrane was stained with Ponceau S for 5-10 min. Subsequently, the transferred proteins and the used size marker were visualized by destaining with distilled water. The bands of the size marker were traced with a ballpen.

1x blotting buffer, pH 8.3
25 mM Tris
192 mM glycine
0.1% (w/v) SDS
10-20% methanol

Ponceau S, pH 8.3
0.2% Ponceau S
3% trichloroacetic acid
3% sulfosalicylic acid

Detection

For visualization of the expected proteins on immunoblots, an enhanced chemiluminescence (ECL) assay was used. ECL is based on the use of luminol and an oxidizing reagent and depends on enzyme-catalyzed production of light: Horse radish peroxidase (HRP) conjugated to the secondary antibody catalyzes the oxidation of luminol in the presence of hydrogen peroxide (H_2O_2) being contained in the oxidizing reagent; thus, light emits and the desired proteins can be detected.

The membrane was pre-incubated in blocking solution at room temperature (RT) in a wet chamber for 30 min. After removing the blocking solution, the membrane was incubated with the first antibody α-AcH3 diluted 1:5000 in blocking solution at 4°C in a wet chamber with gentle agitation o. n.. On the next day the membrane was washed with 1x PBST (3 x 10 min) before the secondary HRP-labeled α-rabbit antibody diluted 1:10 000 in 1x PBST was applied to the membrane for 45-60 min at RT in a wet chamber with gentle agitation. The secondary antibody must not be diluted in blocking solution, because HRP tends to react with NaN_3; hence, the HRP-dependent catalyzation acquired for the light emission would be prevented. After another wash with 1x PBST (3 x 10 min), the membrane was finally treated with a chemoluminescent solution to visualize the HRP conjugates. Therefore luminol and oxidizing reagent (Perkin Elmer) were freshly mixed 1:1 and directly applied to the membrane which was then packed in saran wrap and fixed into an exposure cassette with the protein side up. X-ray films (Kodak) were

exposed to the membrane for 2-15 min, depending on the intensity of the signal and background.

After an additional washing step with 1x PBST (one brief wash, 2 x 10 min), a second and third immunodetection with different primary antibodies (α-AcH4, α-C-terminal H3) were performed under the same conditions. The secondary antibody and its dilution remained the same as described above.

All primary antibodies as well as the secondary antibody were kindly provided by Mag. Dr. Christina Murko.

		Manufacturer	Dilution	Host species
Primary antibodies	α-AcH3	Millipore	1:5000	rabbit
	α-AcH4	Millipore	1:5000	rabbit
	α-C-terminal H3	Abcam	1:20 000	rabbit
Secondary antibody	α-rabbit-HRP	Amersham	1:10 000	

Blocking solution

1x PBS
1% PVP
1% non-fat dry milk
0.1% Tween 20
0.01% NaN_3

1x PBST

1x PBS, pH 7.4
0.1% Tween 20

3. Results

3.1. Histological and morphometric analysis of the treated embryonic hearts

To be able to analyze the effects caused by down-regulation of class I HDACs in the developing hearts of chicken embryos, the hearts were exposed to the histone deacetylase inhibitor TSA during stage HH 23-24 of embryogenesis. The administration of TSA to the chicken hearts was accomplished by implantation of TSA soaked beads or direct injection of the inhibitor; 2 different concentrations of TSA were tested. After reincubation of the embryos, the hearts were removed and photographed. For histological analysis the hearts were fixed, embedded, sectioned and stained; the cell nuclei of the heart tissue were dyed blue and the cytoplasm was counterstained pink. These histological stained sections of the embryonic chicken hearts were examined and photographed. During the microscopic observation of the sections, the most prominent phenotypes being detected were aberrant areal proportions of atria to ventricles and of left ventricle to right ventricle. Therefore the areas of the left and right ventricle and of the atria were the subsequently measured and evaluated features. Additionally, the areas of the whole hearts were measured to be able to compare the sizes of TSA treated hearts and control hearts.

Analyzing the data of the areal measurements of the whole hearts, a hypertrophy of the TSA treated cardiac tissue was evident (Graph 1). Graph 1 shows the combined mean values of the measurements of all examined cardiac tissue, including the hearts after implantation of beads and the hearts after direct injection into the pericardial cavity.

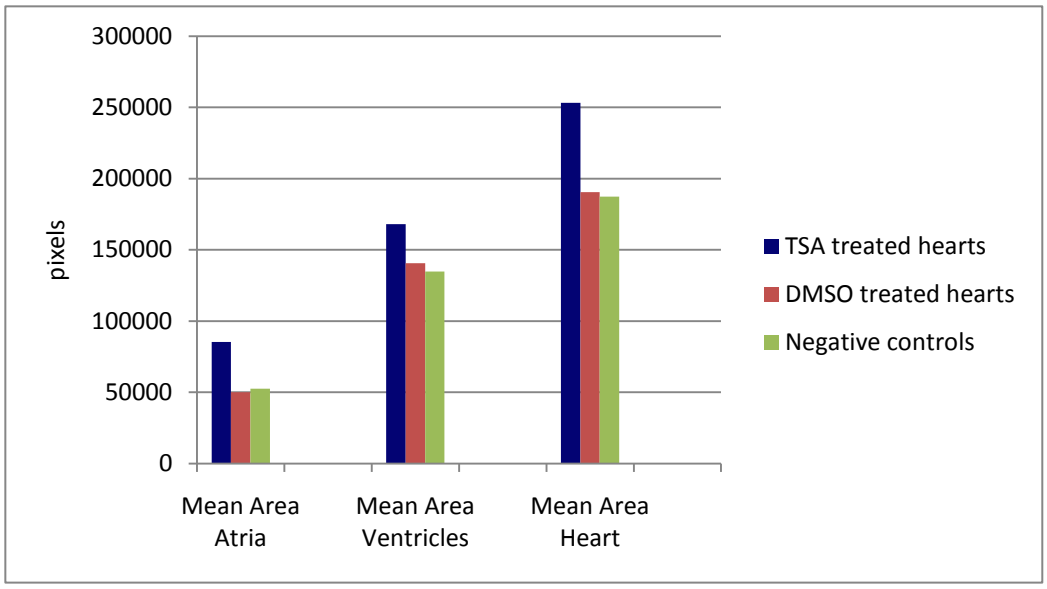

Graph 1: Mean values of the areal measurements of the whole hearts. The analysis included 7 TSA treated hearts (the values of these consist of the measured values of 3 hearts after implantation of beads and of 4 hearts after injection), 4 DMSO treated hearts and 2 untreated hearts. Values are given in pixels.

Interestingly, differences in phenotypic effects were observed after either implantation of beads soaked in the inhibitor or direct injection of TSA into the pericardial cavity.

The TSA treated hearts obtained after implantation of beads displayed an increase in the size of the ventricles and of the atria; the increase in size of the atria was nearly as high as the increase of size of the ventricles (Graph 2). The implantation of beads generates a local source of high TSA concentration and consequently exerts a local effect on the cardiac tissue depending on the site of implantation; thus, each single heart of the implantation series was compared to the mean values of the atrial and ventricular areas of the control hearts. As a result, 50% of the phenotypic alterations were an atrial hypertrophy and 50% of the arisen phenotypes were a ventricular hypertrophy; one of the specimens displayed a severe atrial hypertrophy and, additionally, a slight enlargement of the ventricles. The combination of the individual areal mean values of these hearts resulted in a similar increase in size of atria and ventricles (as seen in Graph 2). Consequently, the variable phenotypes of TSA treated hearts after implantation of beads caused a balanced increase in size of the atrial and the ventricular area.

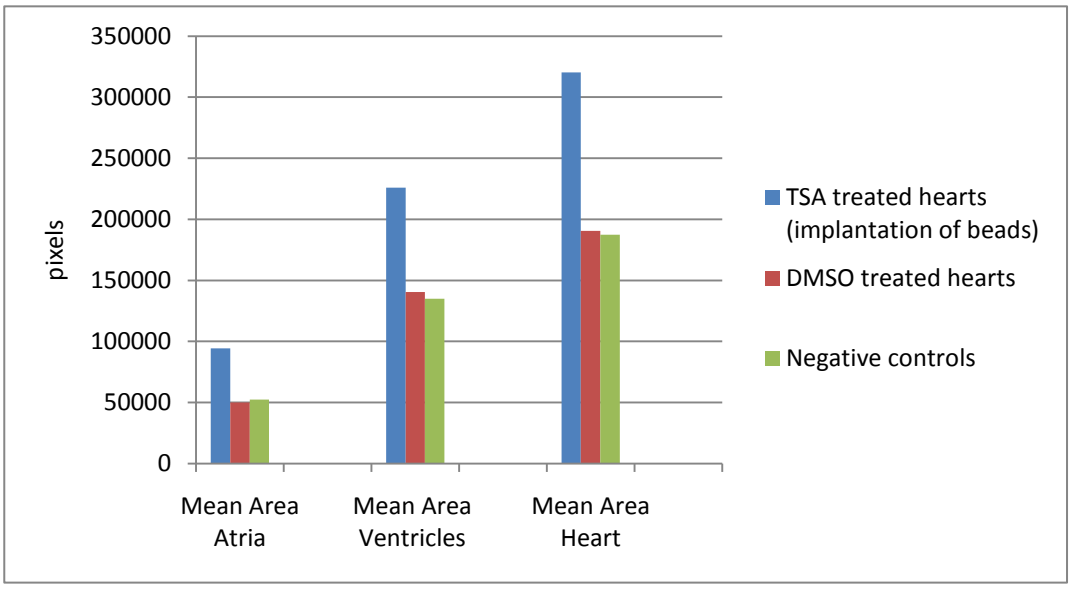

Graph 2: Mean values of the areal measurements of the whole hearts; the TSA treated hearts were exposed to the HDAC inhibitor by implantation of heparin-acrylic beads soaked in TSA. The analysis included 3 TSA (165 µM) treated hearts, 4 DMSO (0.05%) treated hearts and 2 untreated hearts. Values are given in pixels.

The hearts which were exposed to TSA by direct injection showed a clear increase in atrial size and a minimal reduction in the size of the ventricles (Graph 3). In contrast to the implantation of beads, injections result in a homogenous distribution of TSA within the pericardial cavity as judged by homogenous distribution of the co-injected fast green and, thus, seem to generate rather homogeneous phenotypes. Like with the cardiac tissue after implantation of beads, each one of the injected hearts was also compared to the mean values of the atrial and ventricular areas of the control hearts. Every heart displayed an atrial hypertrophy; one specimen was generally smaller than the other measured hearts and, consequently, caused the minimally reduced mean ventricular area of the TSA treated hearts which is apparent in Graph 3. Concerning the injected hearts, the atrial hypertrophy represents a homogeneous phenotype which was even reflected in the areal mean values of the atria and the ventricles of the TSA treated cardiac tissue (Graph 3).

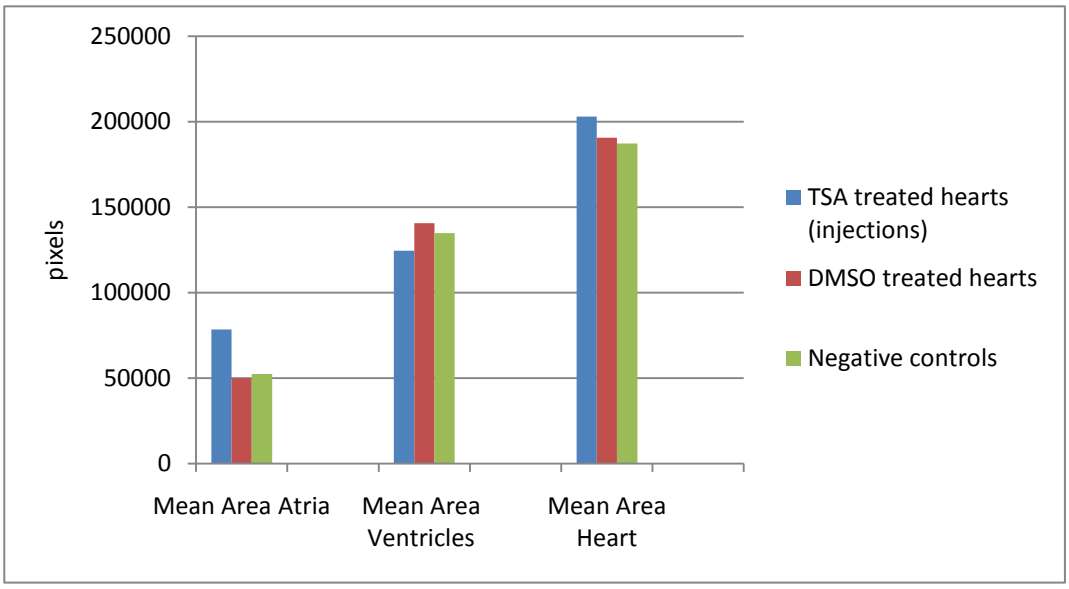

Graph 3: Mean values of the areal measurements of the whole hearts; the TSA treated hearts were exposed to the HDAC inhibitor by direct injection of TSA. The analysis included 4 TSA treated hearts (3 specimens were treated with 50 µM TSA and 1 heart was treated with 165 µM TSA), 4 DMSO (0.05%) treated hearts and 2 untreated hearts. Values are given in pixels.

In total, 57 histological evaluable hearts were observed: 22 hearts were treated with TSA, to 28 hearts DMSO was administered and 7 hearts received no treatment.

The chicken hearts treated with TSA displayed multiple phenotypes. All 5 embryonic hearts affected by implantation of acrylic beads loaded with 165 µM of the HDAC inhibitor showed deviant areal proportions of atria to ventricles; atrial hypertrophy (Fig. 1) was detected in 60% of the cardiac tissue and in 40% ventricular hypertrophy (Fig. 2) was noted. 4 of these hearts revealed several other alterations: Hypertrophy of the right ventricle (Fig. 2) was found in 75% of the hearts, malformations of the ventricular septum (missing septum, inappropriate septation) were observed in 50% of the samples, disturbances in the formation of the outflow tract (incorrect positioning, hypertrophy) were also recognized in 50% and in 25% of the cardiac tissues the sinus venosus was formed notably massive.

The implantation of TSA soaked acrylic beads generated rather heterogeneous phenotypes; as mentioned above, the effect of the beads is assumed to be a local one and to depend on the implantation site and also on the heartbeat, which is able to rearrange the position of the bead. Therefore, the heart area affected by TSA and its association to the observed phenotype is difficult to determine. Injections enable a better distribution of the HDAC inhibitor within the pericardial cavity and are expected to induce more consistent phenotypes. However, the influence of the injected TSA on

the hearts is considered less severe, because injections have no repository qualities and the effects are believed to wash off more quickly.

The first series of TSA injections into the pericardial cavity of the embryonic hearts was performed with a 165 µM solution of the HDAC inhibitor. As a consequence half of the treated embryos died during the 24-hour reincubation time; therefore, 2 different concentrations of TSA, 50 µM and again 165 µM, were tested in the next injection sequence. This time only 3 of 14 TSA treated embryos died; to all 3 of them the 50 µM TSA solution was administered. This lethality is supposed to be due to serious organic damages caused during the injection process. Additionally to the low lethality rate, the hearts derived from the second series displayed milder phenotypes than the ones obtained from the first injection sequence; ~55% of the hearts showed even no phenotype. A possible explanation for the mild phenotypes may be that the stability of TSA reached its limit and the efficacy of the inhibitor weakened.

There was no obvious association between the severity of the phenotype and the injected TSA concentration; both concentrations generated the same severity of phenotypes. Taking the 17 evaluable hearts of the first and the second injection series together, ~35% of the hearts showed no phenotype, in ~41% an atrial hypertrophy (Fig. 3 & 4) was observable, ~12% displayed a hypertrophy of the right ventricle and in 6% respectively ventricular hypertrophy and disturbances in the formation of the outflow tract or incorrect positioning of the atria were detected. 2 of the 7 hearts exhibiting an atrial hypertrophy showed additional malformations: 1 of these hearts missed the ventricular septum and the other one demonstrated an aberrant formation of the outflow tract.

The most prominent phenotypes being detected were aberrant areal proportions of atria to ventricles and of left ventricle to right ventricle; these features were measured and compared to control hearts, which were either treated with DMSO (solvent of TSA) or received no treatment at all.

As the HDAC inhibitor, DMSO was also transferred into the pericardial cavity via implantation of beads soaked in 0.05% DMSO or direct injections being performed with a 0.05% and a 0.015% DMSO solution. In total 28 DMSO hearts were evaluated: ~82% of these control hearts presented no phenotype (Fig. 5) and ~18% revealed a very mild phenotype; 4 hearts displayed an atrial hypertrophy and the ventricles of 1 heart were septated inaccurately. The detected phenotypes were not accumulated in one of the implantation or injection series; they were distributed regularly.

In conclusion, the DMSO hearts demonstrated a very mild phenotype; however, the rate and severity of phenotypes observed in the TSA treated embryonic hearts were much more pronounced.

The 7 untreated hearts were used as negative controls; none of them showed an aberrant phenotype.

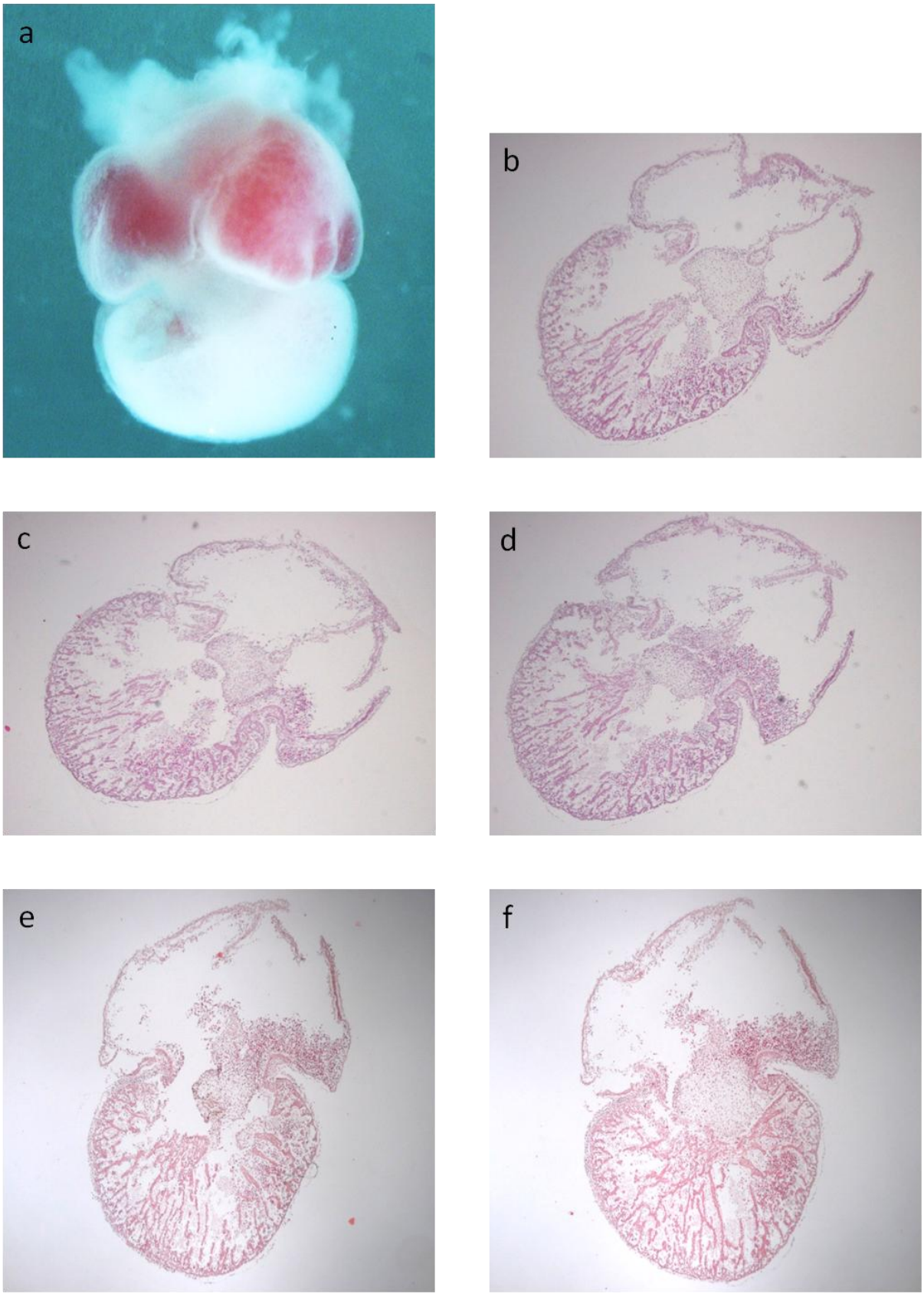

Fig. 1: TSA treated embryonic chicken heart at developmental stage HH 27. The heart was exposed to the HDAC inhibitor by implantation of 2 heparin-acrylic beads soaked in 165 µM TSA. (a) whole heart, (b-f) histological stained sections show deviant proportions of atria to ventricles (atrial hypertrophy).

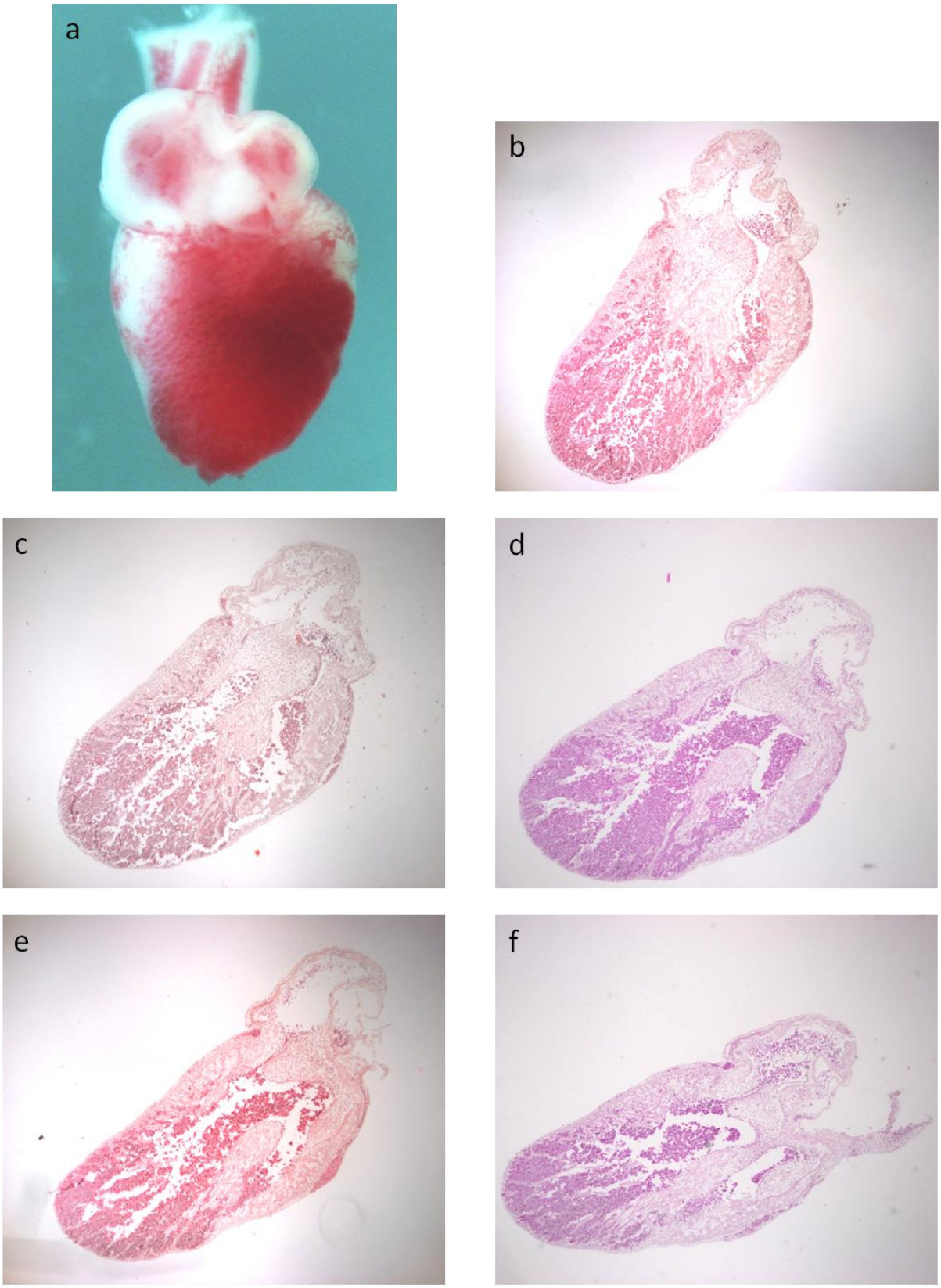

Fig. 2: TSA treated embryonic chicken heart at developmental stage HH 29. The heart was exposed to the HDAC inhibitor by implantation of 4 heparin-acrylic beads soaked in 165 µM TSA. (a) whole heart, (b-f) histological stained sections show deviant proportions of atria to ventricles (ventricular hypertrophy) and of right ventricle to left ventricle (hypertrophy of the right ventricle).

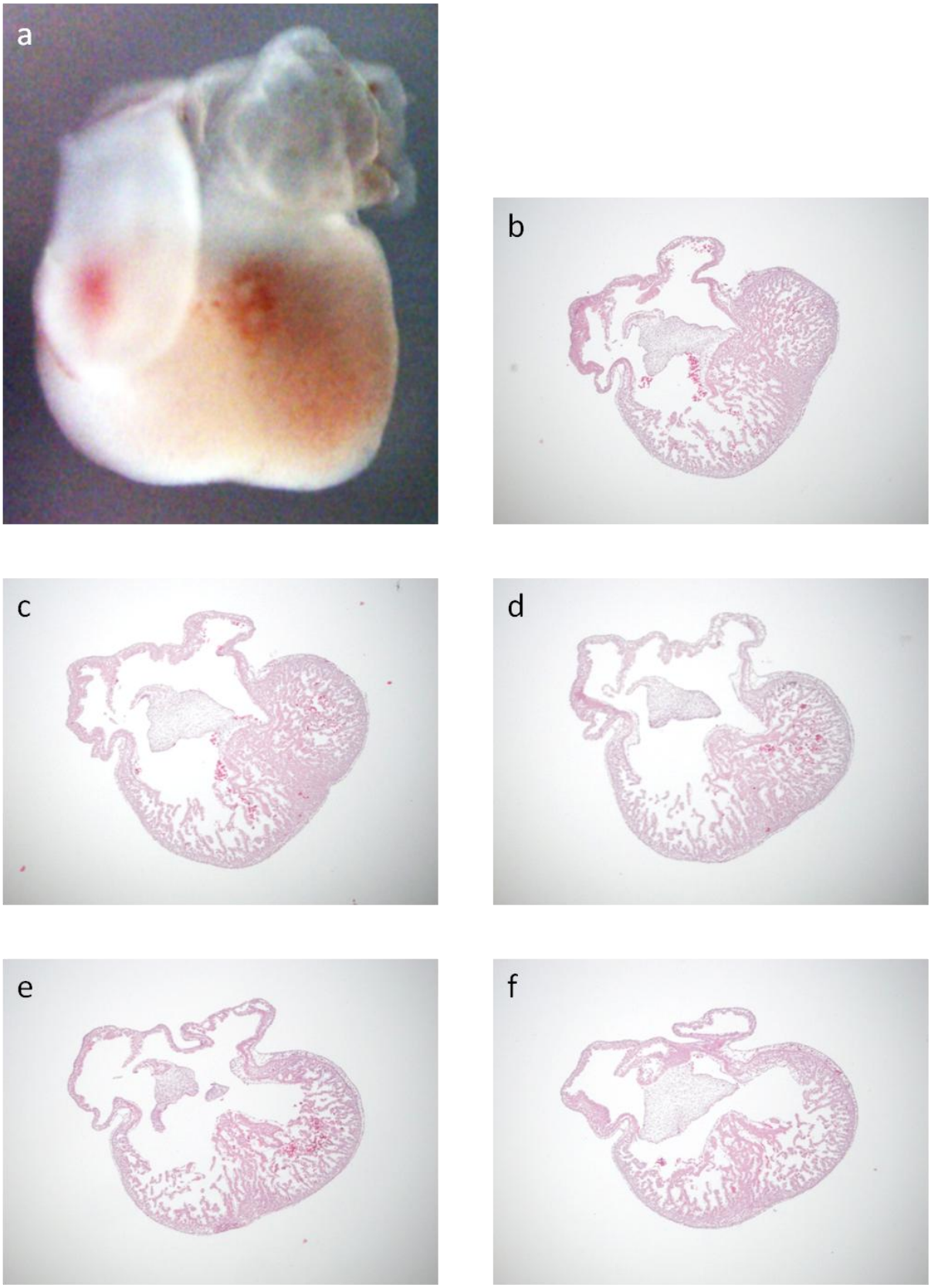

Fig. 3: TSA treated embryonic chicken heart at developmental stage HH 26. The heart was exposed to the HDAC inhibitor by direct injection of 50 µM TSA. (a) whole heart, (b-f) histological stained sections show a mild phenotype of deviant proportions of atria to ventricles (atrial hypertrophy).

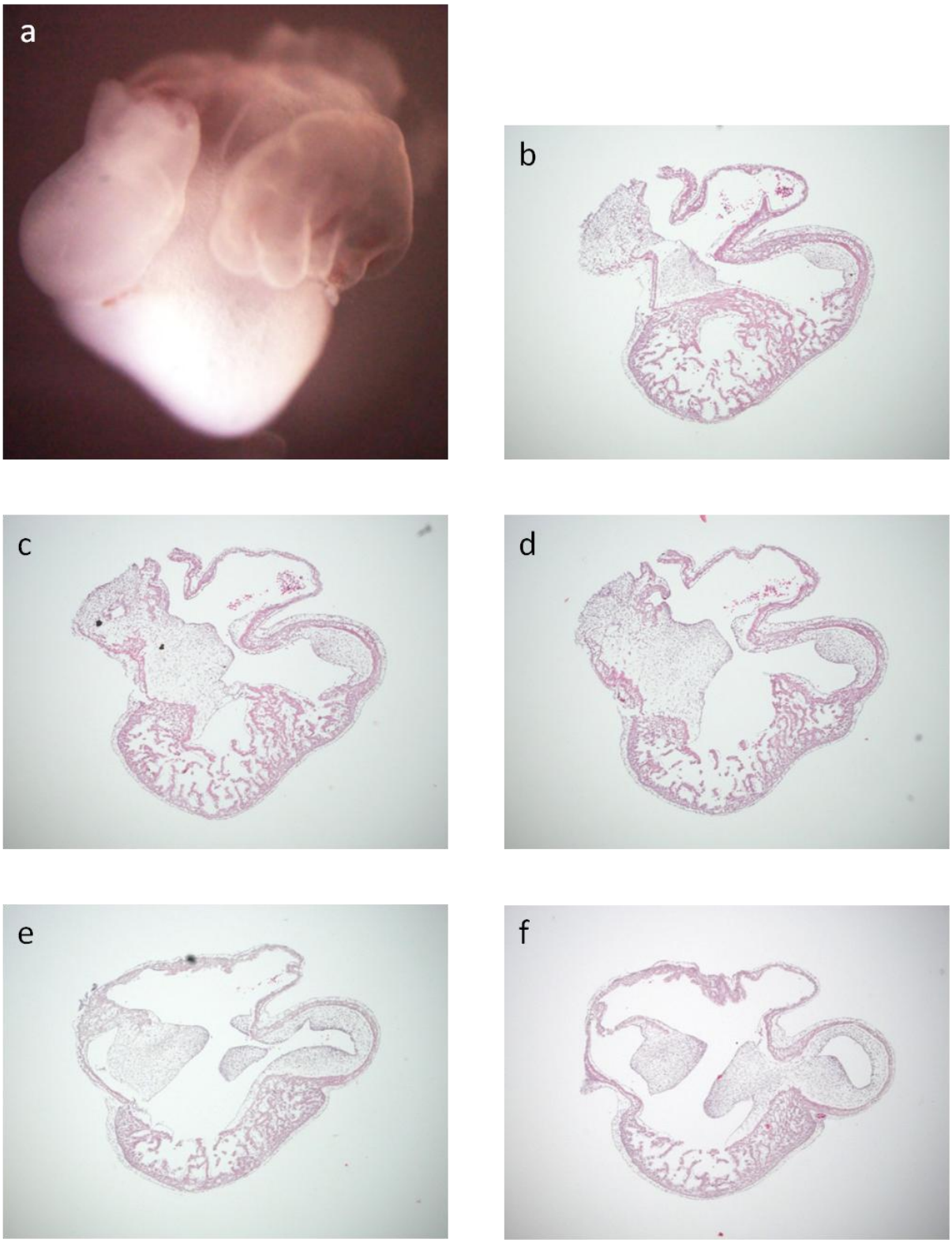

Fig. 4: TSA treated embryonic chicken heart at developmental stage HH 27. The heart was exposed to the HDAC inhibitor by direct injection of 165 µM TSA. (a) whole heart, (b-f) histological stained sections show a mild phenotype of deviant proportions of atria to ventricles (atrial hypertrophy).

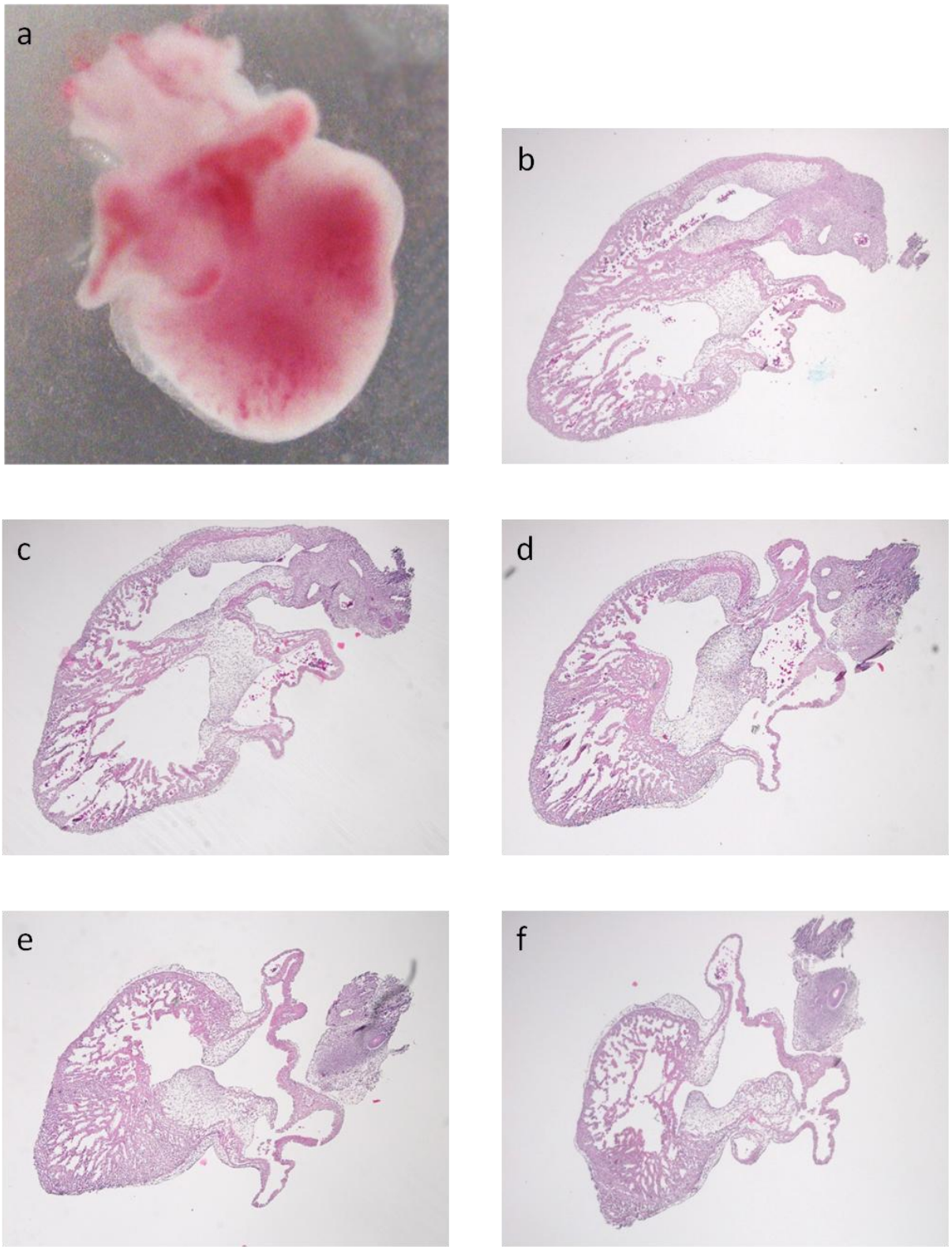

Fig. 5: DMSO treated embryonic chicken heart at developmental stage HH 26. The control heart was exposed to DMSO by implantation of 2 heparin-acrylic beads soaked in 0.05% DMSO. (a) whole heart, (b-f) histological stained sections show no phenotype.

After measuring the areas of the left and right ventricle and of the atria of the TSA and DMSO treated hearts and the untreated cardiac tissue, the data were analyzed.
As previously mentioned, the implantation of TSA beads induced a very local effect, which could be clearly recognized on the cardiac tissue; nevertheless, due to that local effect, these hearts could not be used for adequate morphometric analysis. The hearts of the first injection series were required for determination of the acetylation level of TSA treated hearts; thus, the measurement data of the embryonic hearts of the second sequence of injections remained to be evaluated. Table 1 shows the mean values of the measured and analyzed data.

Treatment of the hearts	Atria:ventricles ratio	Left ventricle:right ventricle ratio
TSA	1:1.6	1:1.3
DMSO	1:2.9	1:1.5
Untreated	1:2.8	1:1.7

Table 1: Mean values of the areal ratios of atria to ventricles and of left ventricle to right ventricle. The analysis included 4 TSA treated hearts, 3 DMSO treated hearts and 2 untreated hearts.

Concerning the atria to ventricles ratio, the TSA treated hearts present a significant difference to the DMSO treated and the untreated hearts; in proportion to the atria, the ventricles of the control hearts are approximately twice as large as the ventricles of the TSA treated hearts. The left ventricle to right ventricle ratio of the TSA treated cardiac tissue demonstrates no significant deviation to the values of the control hearts. Probably, the mildness of the malformation (being common in the second series of TSA injections) and the low percentage representing the addressed phenotype does not affect the mean value.

3.2. Analysis of proliferation and apoptosis in the treated embryonic hearts

To exclude the possibility that TSA and/ or DMSO have caused apoptosis in the embryonic hearts and that, consequently, the phenotypes have to be attributed to apoptotic effects, an apoptosis and a proliferation assay were performed.
For the BrdU cell proliferation assay, the synthetic nucleoside was administered to the embryos 1 h before the hearts were to be removed. After the removal, the hearts were

fixed, embedded in paraffin and sectioned; subsequently, the BrdU assay was performed. Proliferating cells were labeled with Alexa 488, a fluorescent dye emitting green light; after counterstaining with DAPI, the cell nuclei appeared blue under the fluorescent microscope.

The TUNEL assay requires no pre-treatment. Hence, the embryos were removed from the eggs and the chicken hearts were fixed, embedded and sectioned before the TUNEL assay was carried out. Apoptotic cells were labeled with the fluorescent dye fluorescein (FITC), thus, they appeared green under the fluorescent microscope. The cell nuclei were again counterstained with DAPI.

Both assays were performed with sections of the same 11 embryonic chicken hearts being derived from the second series of TSA/ DMSO injections: 3 hearts were treated with 50 µM TSA, to 3 hearts 165 µM TSA was administered, 2 hearts had received 0.05% DMSO injections and 3 hearts had remained untreated.

The evaluated regions were the pericardium, the atrial and ventricular myocardia, the myocardium of the outflow tract and the endocardial cushions.

In these examined cardiac tissues autofluorescent erythrocytes were recognized; these cells were not included in the analysis.

The green Alexa 488 signal of the BrdU assay was clearly perceptible in every sample. Positive cells were detected in the pericardium and in the endocardial cushions, where the signal was distributed almost equally. There were also positive signals detectable in the myocardia of the atria and of both ventricles; in contrast to the previously mentioned structures, these cardiac tissues showed a locally confined proliferation (Fig. 6). Comparing the different treated hearts, the intensity of the signal varied only slightly from heart to heart. Consequently, between TSA-, DMSO-, and untreated hearts, there were no differences in proliferation behavior observable.

Regarding the TUNEL assay, in all hearts the green fluorescein signal was distinctly noticeable in the pericardium and the endocardial cushions (Fig. 7). In some of the hearts positive cells could also be detected in the muscular tissues, but they were found to be only locally restricted. One heart, treated with 165 µM TSA, showed clearly perceptible positive cells for apoptosis in the myocardium of the outflow tract (Fig. 7). A minimal positive signal in the atrial myocardium was observed in a 50 µM TSA treated heart as well as in one of the DMSO treated hearts. A further slight positive staining was identified in the myocardium of the right ventricle of 2 TSA treated hearts (to one of these hearts 165 µM were administered and the other one was treated with 50 µM TSA) and one untreated heart. In another 50 µM treated heart an even fainter signal could be

noticed in the left ventricular myocardium. In short, these locally confined minimal signals in the muscular cardiac tissues were distributed throughout the range of different treated hearts and were not particularly found in TSA-, DMSO- or un-treated hearts; hence, hearts treated with TSA or DMSO were not more apoptotic than untreated hearts.

Comparing these both assays, apoptosis and proliferation did not overlap. In the apoptotic regions of the hearts no enhanced proliferation signal was noticed; apoptosis was not compensated by increased proliferation in the affected areas. Accordingly, in the regions in which a clearly perceptible TUNEL signal was detected, apoptosis was a desired developmental effect: At about stages HH 27-31 in chicken development, the aortico-pulmonary septum dividing the truncus arteriosus in the aorta and the pulmonary artery, is built. During this process, extensive apoptosis and remodelling take place in the myocardium of the outflow tract and facilitate the appropriate positioning of the great vessels over their particular ventricles. (Bellairs & Osmond, 2005)

In the endocardial cushions, there could be found clearly noticeable signals for apoptosis and proliferation. The high intensity of the signals in the cushions could possibly express the remodelling of these structures to septa or valves. The cushions play a vital role in heart septation which occurs about developmental stages HH 24-31. (Bellairs & Osmond, 2005) The observed hearts were removed from the embryo at stages HH 24-27.

Concerning the pericardium, where also distinctly visible signals of proliferation and apoptosis were located, it is possible that the performances of the assays were responsible for the strongly positive cells. During the incubation of the cardiac tissue with the antibodies, coverslips were placed over the sections to prevent them from drying; the antibodies maybe accumulated at the marginal structures of the sections and, thus, the pericardium became stained at such a high level.

The performed assays do not allow a quantitative evaluation of proliferation and apoptosis in whole hearts. Nevertheless, the information given by the BrdU- and the TUNEL assays allow the conclusion that the used concentrations of the HDAC inhibitor and its solvent have not severely affected apoptosis or proliferation in the examined cardiac tissues. In both assays no significant differences between TSA treated cardiac tissues and control hearts were observable. This result confirms the assumption that the detected phenotype of the TSA treated hearts (i. e. the deviant areal proportions of atria to ventricles) is genuinely a hypertrophy signifying an escalated cell size for the same cell

number rather than a hyperplasia, represented by an increased cell proliferation rate without expansion of cell size.

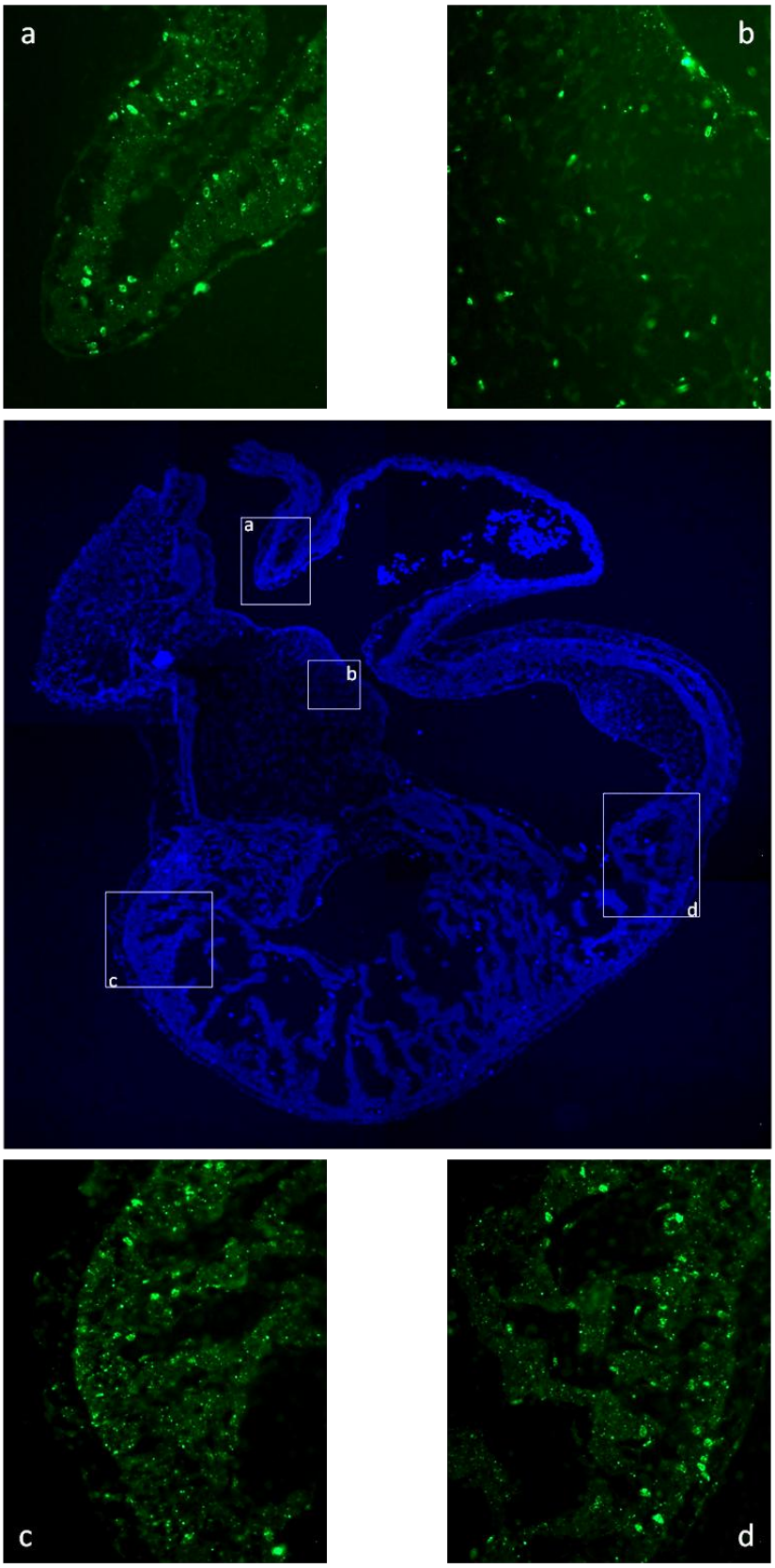

Fig. 6: Proliferation assay of a TSA treated embryonic chicken heart at developmental stage HH 27. The heart was exposed to the HDAC inhibitor by direct injection of 165 µM TSA. (a) atrial myocardium, (b) endocardial cushions, (c) right ventricular myocardium and pericardium, (d) left ventricular myocardium.

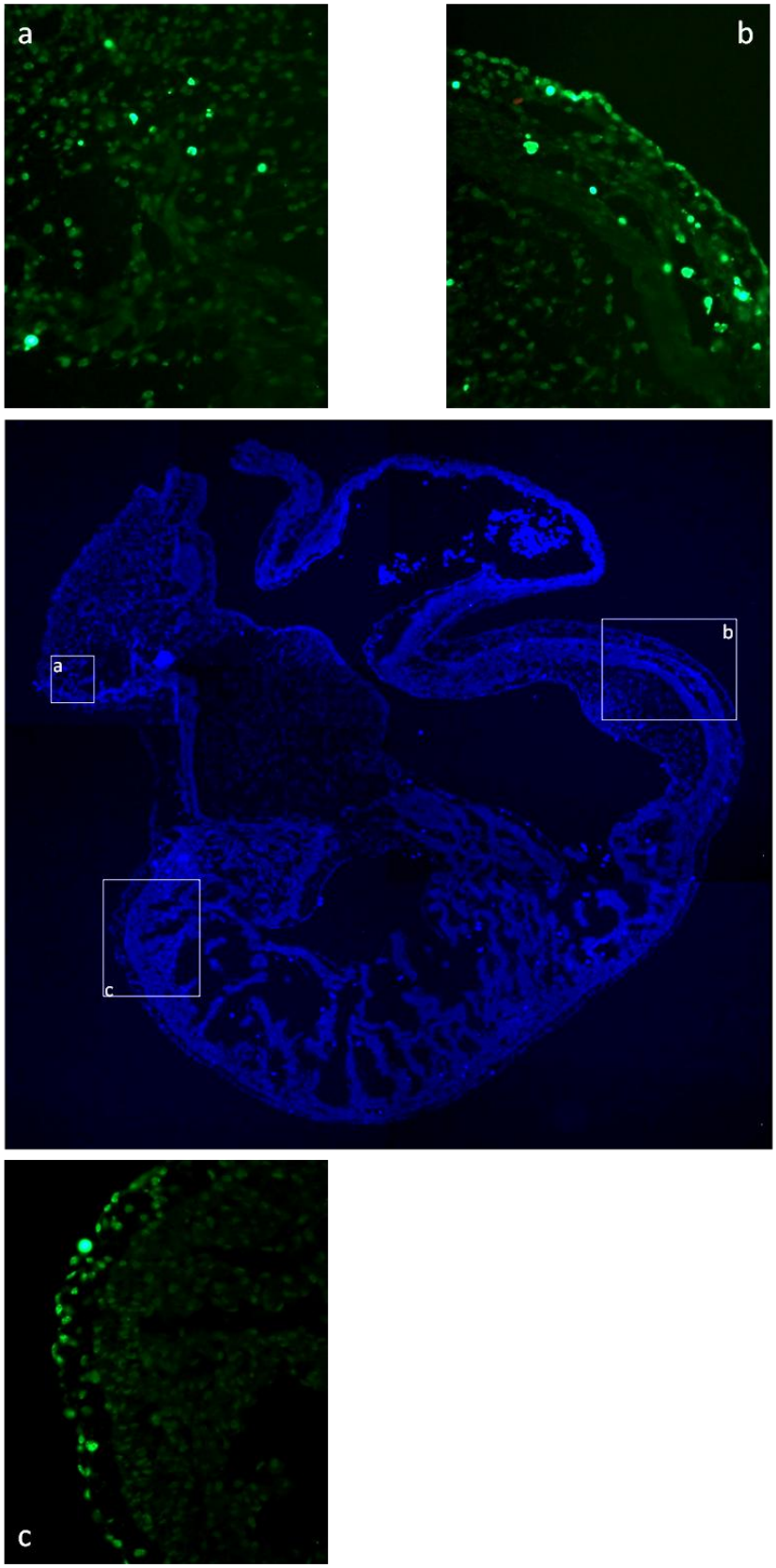

Fig. 7: Apoptosis assay of a TSA treated embryonic chicken heart at developmental stage HH 27. The heart was exposed to the HDAC inhibitor by direct injection of 165 µM TSA. (a) endocardial cushions, (b) myocardium of the outflow tract, (c) pericardium.

3.3. Analysis of the acetylation level of the treated embryonic hearts

To be able to determine the acetylation level of TSA-treated hearts, a Western analysis was carried out. For comparison, DMSO-treated and untreated embryonic hearts were included in the analysis. To maintain the acetylation level of the core histones in the nuclei of the cardiac tissue, the chicken embryos being removed from the eggs, were immediately placed in sodium butyrate; the subsequently extracted hearts were also kept in sodium butyrate. The histones were isolated from the cardiac tissue and separated on SDS gels; 82.5 µg of proteins were loaded on each lane in a total volume of 8 µl. The Coomassie staining of one gel showed that the protein extract contained the expected histones and confirmed that the same quantity of each sample was loaded. The other gel was used for Western analysis; the separated histones were blotted onto a nitrocellulose membrane. The efficiency of the blotting was ensured by Ponceau S staining of the membrane. The detection and visualization of the acetylated histones H3 and H4 was accomplished by immunohistochemistry.

Western analysis was performed twice, once with embryonic chicken hearts being derived from an implantation sequence having used beads soaked in 165 µM TSA or 0.05% DMSO; the second analysis was accomplished with hearts from the first series of injections also having applied 165 µM TSA or 0.05% DMSO to the hearts.

The first Western blot was carried out with hearts of embryos at developmental stages HH 24/25 being gained 6 h after the implantation of beads, and with cardiac tissues of embryos at HH 26/27 which were acquired 24 h after the implantation. The analysis of this first blot showed no differences in the acetylation level of TSA-, DMSO-, or untreated embryonic chicken hearts (Fig. 8). It is supposed that the effect caused by the beads was too locally limited to exert influence on the whole heart.

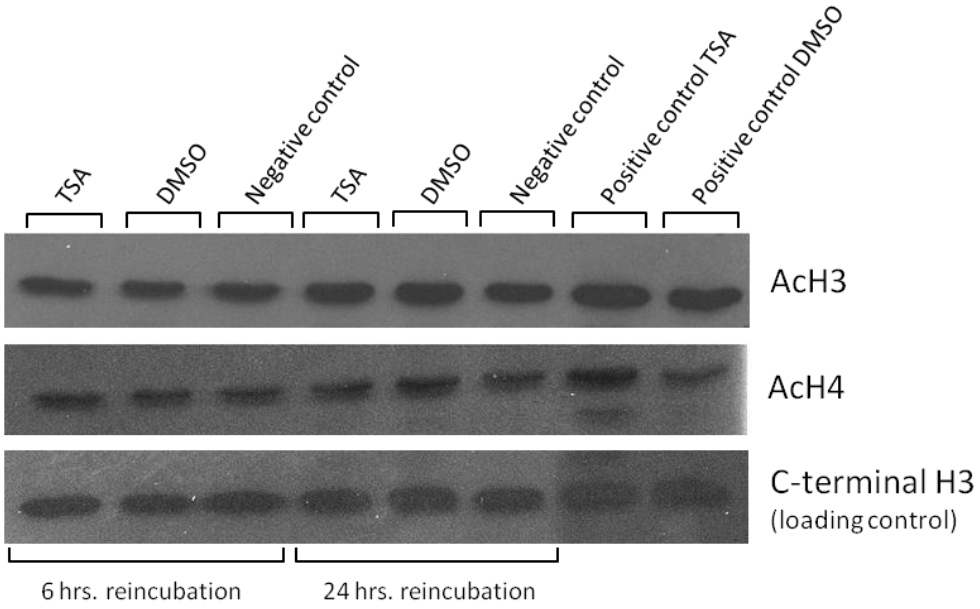

Fig. 8: The histone blot shows the cardiac acetylation level of histones H3 and H4 after 6 h and after 24 h of reincubation. The hearts were treated with TSA (165 µM) or DMSO (0.05%) releasing beads. As negative controls untreated hearts were used. Positive controls for TSA and DMSO were isolated from 293-cells. For the loading control α-C-terminal H3 antibody was used.

The second Western analysis was achieved with cardiac tissues of chicken embryos at stages HH 26/27 which were gained 24 h after the injections. The Ponceau S staining of the nitrocellulose membrane provided information about the efficiency of the blotting process. All desired proteins were transferred successfully onto the membrane. Nevertheless, the band displaying the histones of the DMSO treated hearts was not as intense as the bands showing the histones of the TSA-, and the untreated cardiac tissues; apparently, a too small quantity of proteins was loaded on the gel. Hence, the band of the DMSO treated hearts was excluded from the analysis; this only concerns the DMSO band detected and visualized by the α-AcH4 antibody. Furthermore, difficulties were caused during the detection and visualization procedure; the loading control could not be performed successfully.

The analysis of the hearts treated by injections demonstrated no differences in the acetylation level of histone H3; the bands of the TSA-, DMSO-, and untreated hearts showed the same intensities. As for histone H4, the band of the TSA treated heart displays a higher intensity than the one presenting the untreated negative control (Fig. 9); hence, the hearts to which the histone deacetylase inhibitor was administered appear to have a higher acetylation level for histone H4 than the untreated cardiac tissues.

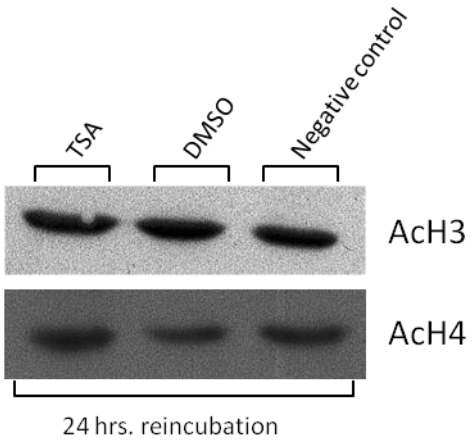

Fig. 9: The histone blot shows the cardiac acetylation level of histones H3 and H4 after 24 h of reincubation. The hearts were treated with TSA (165 µM) or DMSO (0.05%) by injections. As negative controls untreated hearts were used. The DMSO band detected by the α-AcH4 antibody was excluded from the analysis. The loading control, which should have been performed with α-C-terminal H3 antibody, failed.

4. Discussion

This study has addressed the role of class I HDACs in cardiac development of the avian model organism “chicken” during early embryonic stages. Due to previously performed experimentations by Murko and colleagues (2010), the temporal expression patterns of *Hdacs 1, 2, 3*, and *8* in the chick heart were known. Thus, to gain insight into the roles of class I HDACs in the cardiac tissue, these enzymes were inhibited by TSA. Subsequent histological and morphometric analysis, a proliferation assay as well as an apoptosis assay, and the determination of the acetylation level in the chick hearts allowed first observations of the phenotypic effects of class I HDAC inhibition in avian cardiac tissue. The examined chicken hearts treated with the HDAC inhibitor displayed a range of severe phenotypes, such as atrial hypertrophy, ventricular hypertrophy, hypertrophy of the right ventricle, malformations of the ventricular septum, and aberrant formation of the outflow tract. However, the cardiac tissue showing hypertrophic effects, especially atrial hypertrophy, was found to be more pronounced than the other phenotypes.

It should be noted that TSA also depletes class II HDACs (HDACs 4 to 7, 9, and 10) (Zhao et al., 2009); thus, the observed cardiac hypertrophy could also be due to the activities of class II HDACs.

Cardiac hypertrophy, signified by an escalated cell size for the same cell number, is a result of cardiomyocytes responding to stress signals; multiple extracellular agonists (e. g. α- and β-adrenergic agonists, endothelin, angiotensin, and 5-hydroxytryptamine), intensified cardiac workload, cell stretch, and aberrant sarcomeric structure and function cause hypertrophic growth of cardiac myocytes. At the cellular level, the hypertrophic response is typically characterized by an enlarged size of cardiac cells, an intensified protein synthesis, an altered formation of sarcomeres, and reactivation of a fetal gene program being responsible for the reduced efficiency of the heart. (Backs & Olson, 2006) Stress-induced hypertrophy is meant to compensate ventricular wall stress; however, if the hypertrophic growth of cardiomyocytes persists, the subsequent enlargement of the heart results in cardiac arrhythmias, heart failure, and sudden death (Frey & Olson, 2003).

The maintenance of appropriate cardiomyocyte size depends on the balance between pro- and antihypertrophic pathways (Kook et al., 2003). In general, class I HDACs are communicated to repress antihypertrophic genes, whereas class II HDACs are supposed to inhibit the expression of prohypertrophic genes (Backs & Olson, 2006; Kook, et al., 2003).

Cardiac hypertrophy is an often reported phenotype caused by experimentations with mice. For the lack of studies concerning the model organism “chicken” and the high homology between full length proteins of class I HDACs in chicken and mouse (i. e. HDAC1 93.1%, HDAC2 97.8%, HDAC3 96.9%, and HDAC8 87.8%) (Murko et al., 2010), it is assumed that the already known murine cardiac phenotypes can be inferred on the observed hypertrophic effect in embryonic chick hearts. Thus, the possible functions of HDACs in the heart of early chicken embryos related to hypertrophy will be discussed by reference to the previously detected phenotypes of the mouse heart.

By using hypertrophic stimuli, Montgomery et al. (2007) found cardiac hypertrophy in hearts of 8 to 10 week old mice bearing a cardiac deletion of either *Hdac1* or *Hdac2* or of both genes. However, the observed hypertrophic response of these hearts was comparable to the hypertrophic response recognized in the cardiac tissue of wild-type littermates (Montgomery et al., 2007). Trivedi and colleagues (2007) also tested hypertrophic stimuli on postnatal mice carrying a *Hdac2* gene-trap deletion; these mice showed no signs of a cardiac hypertrophic response or a reactivation of the fetal gene program which is typically associated with hypertrophy of the heart (Trivedi et al., 2007). Kee et al. (2008) administered hypertrophic stimuli to hearts of postnatal wild-type mice; a raised activity was discovered for *Hdac2*, but not for *Hdac1*. Furthermore, the activation of *Hdac2* to stimuli causing hypertrophy was tested in cardiomyocytes of neonatal rats which were transiently transfected with wild-type *Hdac2*; the application of the stimuli to the transfected cardiac cells resulted in an escalated *Hdac2* activity. HDAC2 was found to induce the expression of atrial natriuretic factor (ANF) which is a marker of hypertrophy; cardiomyocytes transfected with wild-type *Hdac2* displayed an extended cell size and a stress-induced formation of muscle fibers. An enzymatically inactive form of HDAC2 failed to activate a hypertrophic response. (Kee et al., 2008)

HDAC2 was found to interact with the homeodomain-only protein (HOP), which regulates cardiomyocyte proliferation and growth. An association of HDAC2 and HOP is reported to transcriptionally repress antihypertrophic genes leading to cardiac hypertrophy which was observed 3 weeks after the mice’ birth. Overexpression of a mutant form of HOP which did not recruit HDAC2 prevented hypertrophy of the mouse heart; the deficiency of HDACs caused by inhibitors, such as TSA, also suppress hypertrophic pathways. (Kook et al., 2003) Conversely, in mice a cardiac-specific overexpression of either *Hdac1* or *Hdac2* displayed a robust hypertrophy and dilatation of the heart inducing lethality (Montgomery et al., 2008; Trivedi et al., 2007).

Taken together, these findings support, or at least do not refute, the assumption of class I HDACs being repressors of antihypertrophic genes. However, *Hdac2* expression was not found in the cardiac tissue of the developing chicken embryo (Murko et al., 2010); thus, it remains to be elucidated, if the communicted redundancy of HDACs 1 and 2 enables HDAC1 to compensate for the absence of HDAC2 or if other HDAC related mechanisms underlie the hypertrophic response in chicken hearts.

In contrast to HDACs 1 and 2, HDAC3 is assumed to prevent cardiac hypertrophy. A conditional deletion of *Hdac3* in a mouse heart resulted in a severe hypertrophy with enlarged right and left atria and interstitial fibrosis (designated by fibroblast proliferation causing an increased production of collagen) leading to lethality 3 to 4 month after birth. As for the hypertrophic cardiomyocytes, HDAC3 was found to repress the peroxisome proliferator-activated receptor alpha (PPARα) which operates as a transcription factor regulating the expression of genes involved in fatty-acid intake and metabolism. In *Hdac3*-deficient murine cardiomyocytes, the acetylation levels at the promoters of various PPAR-responsive genes were discovered to be escalated. This increased activity of PPAR-responsive genes caused a ligand-induced accumulation of lipids within the heart ending in lethality after 3-4 month after birth. In addition, several markers indicating cardiac hypertrophy were significantly upregulated and the sarcomeric organization was disrupted leading to minimized contractility and malfunctioning of the ventricles. (Montgomery et al., 2008)

The over-expression of *Hdac3* in murine cardiomyocytes prevented hypertrophy; instead, proliferation of cardiac cells was induced and resulted in enhanced thickness of the myocardium (Trivedi et al., 2008).

In conclusion, compared to HDACs 1 and 2, HDAC3 reveals an exclusive role in the progression of cardiac hypertrophy. The actions of this enzyme seem to argue against a general role of class I HDACs in repressing antihypertrophic genes in cardiac myocytes.

HDAC8 was demonstrated to interact with the estrogen-related receptor α (ERRα) in vivo; the enzyme enhanced the transcriptional function of ERRα (Wilson et al., 2010) regulating genes which encode for enzymes being involved in the maintenance of energy balance in animals. In mice ERRα was found to be expressed at a high level in cardiac tissue (Ranhotra, 2009; Stein & McDonnell, 2006); ERRα controls numerous pathways of mitochondrial energy metabolism in cardiomyocytes (Huss et al., 2007). Huss et al. (2007) showed that the expression of the ERRα gene was diminished in hypertrophic cardiac tissue of mice 10 to 12 weeks of age; the hypertrophy was accompanied by decreased high-energy phosphate supplies and aberrations in glucose

metabolism. In hearts deficient for ERRα, genes associated with oxidation of fatty acids and glucose and such anticipating in phosphate transfer were negatively affected; respiration studies determined a reduced ATP synthesis/O_2 consumption ratio in murine ERRα-null hearts. (Huss et al., 2007)

As previously mentioned, HDAC8 heightens the transcriptional activation of several genes by deacetylating ERRα (Wilson et al., 2010) which is definitely present in cardiac tissue of mice (Ranhotra, 2009; Stein & McDonnell, 2006). If *Hdac8* is expressed in the mammalian heart remains to be fully elucidated for there exist contradictory outcomings (Buggy et al., 2000; Hu et al., 2000; Van den Wyngaert et al., 2000; Waltregny et al., 2004). However, in chicken hearts HDAC8 was detected at low levels by WMISH (Murko et al., 2010). Hence, it may be possible that HDAC8 plays an indirect role in the energy metabolism of avian cardiac tissue via transcriptional regulation of ERRα. In that case, a deletion of *Hdac8* which leads to reduced activity of ERRα (Wilson et al., 2010) should be assumed to cause hypertrophic effects as described for ERRα-deficient mice; thus, as HDAC3, HDAC8 would not act as repressor of antihypertrophic genes. However, if a HDAC8-ERRα-interaction exists in chicken, remains to be elucidated.

Class II HDACs are believed to suppress postnatal hypertrophy of cardiac myocytes (Zhang et al., 2002) by inhibiting expression of prohypertrophic genes (Backs & Olson, 2006; Kook, et al., 2003). Importantly, class IIa HDACs (i. e. HDACs 4, 5, 7, and 9) are reported of being highly redundant (Haberland et al., 2008).

Hypertrophic response in animal hearts bearing a deletion of a member of the class IIa HDAC family is associated with superactivation of myocyte enhancer factor-2 (MEF2) (Zhang et al., 2002); a correlation between the transcription factor MEF2 and cardiac hypertrophy is proposed (Backs & Olson, 2006). Class IIa HDACs are able to interact directly with MEF2 leading to transcriptional repression of genes containing binding sites for MEF2 (Backs & Olson, 2006; Han et al., 2005). MEF2 acts as a calcium-dependent regulator of cell division, differention, and apoptosis; furthermore, MEF2 represents a final target for stress-induced signals in the adult myocardium and is responsible for the activation of fetal gene programs in the heart (McKinsey et al., 2002). Concerning cardiac abnormalities in mice, HDAC5 and HDAC9 are reported to play essential roles. Most of the mice lacking both, *Hdacs 5* and *9*, show severe aberrations of the heart; due to thin-walled myocardium and defects of the ventricular septum the murine embryos die during late stages of development. (Backs & Olson, 2006; Chang et al., 2004; Haberland et al., 2008) Animals being deficient for either *Hdac5* or *Hdac9* are viable and display no cardiac phenotype at early age; however, at about 6 months after birth, in the

mutant mice a hypertrophy of the heart was established spontaneously (Chang et al., 2004). Mice lacking either of these both enzymes developed a hypersensitivity to stress-dependent signals, such as caused by age-related cardiac insults. In the myocardium of wild-type hearts stress stimuli usually activate the calcineurin (CN) and calmodulin dependent protein kinase (CaMK)-protein kinase D (PKD) pathways resulting in phosphorylation of the class IIa HDACs; the phosphorylation leads to export of the HDACs from the cell nucleus to the cytoplasm. Besides the inactivation of class IIa HDACs by nuclear export, a Ca^{2+}/calmodulin (CaM) complex interacts with class IIa HDACs, thereby replacing MEF2. Thus, the transcription factor MEF2, which is generally suppressed by class IIa HDACs becomes derepressed and activates genes involved in cellular growth. In a mouse heart bearing a deletion of either *Hdac5* or *Hdac9* the counter-regulatory mechanism inhibiting hypertrophic response of cardiomyocytes is lost; hence, these hearts are hypersensitive to cardiac stress, although the two enzymes acquire redundant roles in the repression of cardiac hypertrophy in response to stress-induced signals. (Backs & Olson, 2006; Chang et al., 2004; Haberland et al., 2008) Indeed, class IIa HDAC activity is not restricted to repressing MEF2; class IIa HDACs are also able to, directly or indirectly, bind to and inhibit other transcription factors associated with the hypertrophic response in cardiomyocytes (Backs & Olson, 2006).

It is concluded that HDAC5 and HDAC9 repress a distinct subset of hypertrophic signaling pathways being based on intracellular calcium signaling (Backs & Olson, 2006; Chang et al., 2004).

Moreover, besides the repression of MEF2 by class IIa HDACs, class I HDACs are also recruited to suppress MEF2 target genes. Cabin 1 is a further transcriptional repressor of MEF2; Cabin 1 binds MEF2 and inhibits the actions of the transcription factor by recruitment of the mSin3 corepressor and its associated HDACs 1 and 2. (Youn & Liu, 2000)

In addition, HDAC3 has been found out to control MEF2 activity by directly associating and, thus, repressing MEF2 (Grégoire et al., 2007). Furthermore, class II HDACs are reported to obtain no intrinsic deacetylase activity; instead, the addressed HDACs recruit the SMRT/N-CoR-HDAC3 complex to be able to deacetylate and suppress transcription (Fischle et al., 2002). Accordingly, Backs and Olson (2006) consider it likely that class II HDACs recruit the deacetylase activity of class I HDACs which enables the members of class II HDACs to completely apply their repressive exertion on target genes (Backs & Olson, 2006).

In short, cardiac hypertrophy is the result of an entangled complexity of stress tansmitting signaling pathways in which HDACs are definitely involved (Frey & Olson, 2003).

The roles of the other class IIa HDACs (HDACs 4 and 7) and class IIb HDACs (HDAC6 and HDAC10) in cardiac tissue remain to be investigated.

This study has addressed the role of class I HDACs in early avian cardiac development; after inhibition of the HDACs by TSA, significant hypertrophic effects in chicken embryonic hearts were found in vivo. Hence, class I HDACs, and apparently class II HDACs as well, play an important role in cardiac development of early chicken embryos. Interestingly, all investigations concerning cardiac malformations in mice report about postnatal hypertrophy of the heart, whereas in chicken the cardiac hypertrophic effects were already observable at embryonic stages HH26 to HH29 (about 5 to 6 days after incubation). Additionally, in the avian model system the most pronounced cardiac phenotype was an atrial hypertrophy, not a hypertrophy of the whole heart. However, it cannot be ruled out that the enlargement of the atria is only the beginning of a hypertrophy of the whole organ; maybe this is a mechanism to maintain efficient functioning of the ventricles as long as possible and, thus, prolonging heart failure.

To gain additional insight into the activities of class I HDACs in cardiac development of chicken embryos, further studies have to be performed. Morphometric analysis could be extended; the thickness of ventricular and atrial myocardia and septa should be measured to be able to discover more phenotypical differences between TSA treated and control hearts. The formation of the outflow tract should also be given more attention. Another worthy goal is the determination of the spatio-temporal expression patterns of class II HDACs in chicken embryos. To be able to distinguish between the different roles of HDACs during heart development, the enzymes have to be inhibited individually.

However, the experimentations presented in this study were performed in embryonic chicken hearts for the first time. I hope this piece of work provides possibilities for the development of novel manipulation procedures regarding the model system “chicken”.

Acknowledgments

I want to express my appreciation to everybody who gave me technical and scientific as well as personal support to succeed in writing this Diploma thesis.
I want to thank my unofficial supervisor Ao. Univ.-Prof. Dr. Christian Schöfer for inviting me to write on my Diploma thesis in his lab group and for the possibility to study a really interesting topic and the support during the whole thesis.
Moreover, I am grateful to my “technical support” Ing. Marlene Almeder and Mag. Dr. Christina Murko for helping me out in the lab, for all the time they had for me and my questions and for all the patience and good advices.
I also want to say thank you to my official supervisor Ao. Univ.-Prof. Mag.rer.nat. Mag.phil. Dr.rer.nat. Sylvia Kirchengast for supporting me with the whole bureaucracy paving the way to graduation and for being available all the time when questions arose.

Furthermore, I appreciate all my lab colleagues at the Department for Cell and Developmental Biology (Center for Anatomy and Cell Biology, Medical University Vienna) for the great social environment, for their moral support during hard times as well as for the great parties.
I am also really grateful to my family, especially to my sister, and to all my friends for supporting me during troublesome periods. Best thanks to my long-standing and very good friend Claudia for giving me the opportunity for all my studies in biology and supporting me for more than ten years in any situation.

References

Allis, C. D., Jenuwein, T., & Reinberg, D. (Eds.). (2009). *Epigenetics* (Paperback ed.). New York: Cold Spring Harbor Laboratory Press.

Almouzni, G., Khochbin, S., Dimitrov, S., & Wolffe, A. P. (1994). Histone acetylation influences both gene expression and development of Xenopus laevis. *Developmental Biology (165)* , pp. 654-669.

Backs, J., & Olson, E. N. (2006). Control of cardiac growth by histone acetylation/deacetylation. *Circulation Research (98)* , pp. 15-24.

Bellairs, R., & Osmond, M. (2005). *The atlas of chick development* (2nd ed.). London: Elsevier Academic Press.

Branch, D. R., Calderwood, S., Cecuiti, M. A., Herst, R., & Solh, H. (1994). Hematopoietic progenitor cells are resistant to dimethyl sulfoxide toxicity. *Transfusion (34)* , pp. 887-890.

Brunmeir, R., Lagger, S., & Seiser, C. (2009). Histone deacetylase 1 and 2-controlled embryonic development and cell differentiation. *The International Journal of Developmental Biology (53)* , pp. 275-289.

Buggy, J. J., Sideris, M. L., Mak, P., Lorimer, D. D., McIntosh, B., & Clark, J. M. (2000). Cloning and characterization of a novel human histone deacetylase, HDAC8. *Biochemical Journal (350)* , pp. 199-205.

Chang, S., McKinsey, T. A., Zhang, C. L., Richardson, J. A., Hill, J. A., & Olson, E. N. (2004). Histone deacetylases 5 and 9 govern responsiveness of the heart to a subset of stress signals and play redundant roles in heart development. *Molecular and Cellular Biology (24)* , pp. 8467-8476.

Chiba, T., Yokosuka, O., Fukai, K., Kojima, H., Tada, M., Arai, M., et al. (2004). Cell growth inhibiton and gene expression induced by the histone deacetylase inhibitor, Trichostatin A, on human hepatoma cells. *Oncology (66)* , pp. 481-491.

Da Violante, G., Zerrouk, N., Richard, I., Provot, G., Chaumeil, J. C., & Arnaud, P. (2002). Evaluation of the cytotoxicity effect of dimethyl sulfoxide (DMSO) on Caco2/TC7 colon tumor cell cultures. *Biological & Pharmaceutical Bulletin (25)* , pp. 1600-1603.

Escaffit, F. (2007, August). *HDAC3 (Histone deacetylase 3)*. Retrieved January 25, 2011, from Atlas of Genetics and Cytogenetics in Oncology and Haematology: http://AtlasGeneticsOncology.org/Genes/HDAC3ID40804ch5q31.html

Farooq, M., Sulochana, K. N., Pan, X., To, J., Sheng, D., Gong, Z., et al. (2008). Histone deacetylase 3 (hdac3) is specifically required for liver development in zebrafish. *Developmental Biology (317)* , pp. 336-353.

Fischle, W., Dequiedt, F., Hendzel, M. J., Guenther, M. G., Lazar, M. A., Voelter, W., et al. (2002). Enzymatic activity associated with class II HDACs is dependent on a multiprotein complex containing HDAC3 and SMRT/N-CoR. *Molecular Cell (9)* , pp. 45-57.

Frey, N., & Olson, E. N. (2003). Cardiac hypertrophy: the good, the bad, and the ugly. *Annula Review of Physiology (65)* , pp. 45-79.

Grégoire, S., Xiao, L., Nie, J., Zhang, X., Xu, M., Li, J., et al. (2007). Histone deacetylase 3 interacts with and deacetylates myocyte enhancer factor 2. *Molecular and Cellular Biology (27)* , pp. 1280-1295.

Gregoretti, I. V., Lee, Y. M., & Goodson, H. V. (2004). Molecular evolution of the histone deacetylase family: functional implications of phylogenetic analysis. *Journal of Molecular Biology (338)* , pp. 17-31.

Haberland, M., Mokalled, M. H., Montgomery, R. L., & Olson, E. N. (2009). Epigenetic control of skull morphogenesis by histone deacetylase 8. *Genes & Development (23)* , pp. 1625-1630.

Haberland, M., Montgomery, R. L., & Olson, E. N. (2008). The many roles of histone deacetylases in development and physiology: implications for disease and therapy. *Nature Reviews Genetics (advance online publication)* , pp. 1-11.

Hamburger, V., & Hamilton, H. L. (1951). A series of normal stages in the development of the chick embryo. *Journal of Morphology (88)* , pp. 49-92.

Han, A., He, J., Wu, Y., Liu, J. O., & Chen, L. (2005). Mechanism of recruitment of class II histone deacetylases by myocyte enhancer factor-2. *Journal of Molecular Biology (345)* , pp. 91-102.

Hoshikawa, Y., Kwon, H. J., Yoshida, M., Horinouchi, S., & Beppu, T. (1994). Trichostatin A induces morphological changes and gelsolin expression by inhibiting histone deacetylase in human carcinoma cell lines. *Experimental Cell Research (214)* , pp. 189-197.

Hu, E., Chen, Z., Fredrickson, T., Zhu, Y., Kirkpatrick, R., Zhang, G. F., et al. (2000). Cloning and characterization of a novel human class I histone deacetylase that functions as a transcription repressor. *The Journal of Biological Chemistry (275)* , pp. 15254-15264.

Huss, J. M., Imahashi, K. I., Dufour, C. R., Weinheimer, C. J., Courtois, M., Kovacs, A., et al. (2007). The nuclear receptor ERR alpha is required for the bioenergetic and functional adaptation to cardiac pressure overload. *Cell Metabolism (6)* , pp. 25-37.

Jenuwein, T., & Allis, C. D. (2001). Translating the histone code. *Science (293)* , pp. 1074-1080.

Kee, H. J., Eom, G. H., Joung, H., Shin, S., Kim, J. R., Cho, Y. K., et al. (2008). Activation of histone deacetylase 2 by inducible heat shock protein 70 in cardiac hypertrophy. *Circulation Research (103)* , pp. 1259-1269.

Knutson, S. K., Chyla, B. J., Amann, J. M., Bhaskara, S., Huppert, S. S., & Hiebert, S. W. (2008). Liver-specific deletion of histone deacetylase 3 disrupts metabolic transcriptional networks. *The EMBO Journal (27)* , pp. 1017-1028.

Kook, H., Lepore, J. J., Gitler, A. D., Min Lu, M., Wing-Man Yung, W., Mackay, J., et al. (2003). Cardiac hypertrophy and histone deacetylase-dependent transcriptional repression mediated by the atypical homeodomain protein Hop. *The Journal of Clinical Investigation (112)* , pp. 863-871.

Kuwahara, K., Saito, Y., Takano, M., Arai, Y., Yasuno, S., Nakagawa, Y., et al. (2003). NRSF regulates the fetal cardiac gene program and maintains normal cardiac structure and function. *The EMBO Journal (22)* , pp. 6310-6321.

Lagger, G., O'Carroll, D., Rembold, M., Khier, H., Tischler, J., Weitzer, G., et al. (2002). Essential function of histone deacetylase 1 in proliferation control and CDK inhibitor repression. *The EMBO Journal (21)* , pp. 2672-2681.

Lein, E. S., Hawrylycz, M. J., Ao, N., Ayres, M., Bensinger, A., Bernard, A., et al. (2007). Genome-wide atlas of gene expression in the adult mouse brain. *Nature (445)* , pp. 168-176.

Ma, P., & Schultz, R. M. (2008). Histone deacetylase 1 (HDAC1) regulates histone acetylation, development, and gene expression in preimplantation mouse embryos. *Developmental Biology (319)*, pp. 110-120.

MacDonald, J., & Roskams, A. (2008). Histone deacetylases 1 and 2 are expressed at distinct stages of neuro-glial development. *Developmental Dynamics (237)* , pp. 2256-2267.

Malinin, T. I., & Perry, V. P. (1967). Toxicity of dimethyl sulfoxide on HeLa cells. *Cryobiology (4)* , pp. 90-96.

McKinsey, T. A., Zhang, C. L., & Olson, E. N. (2002). MEF2: a calcium-dependent regulator of cell division, differentiation and death. *Trends in Biochemical Sciences (27)* , pp. 40-47.

Montgomery, R. L., Davis, C. A., Potthoff, M. J., Haberland, M., Fielitz, J., Qi, X., et al. (2007). Histone deacetylases 1 and 2 redundantly regulate cardiac morphogenesis, growth, and contractility. *Genes & Development (21)* , pp. 1790-1802.

Montgomery, R. L., Potthoff, M. J., Haberland, M., Qi, X., Matsuzaki, S., Humphries, K. M., et al. (2008). Maintenance of cardiac energy metabolism by histone deacetylase 3 in mice. *The Journal of Clinical Investigation (118)* , pp. 3588-3597.

Murko, C., Lagger, S., Steiner, M., Seiser, C., Schoefer, C., & Pusch, O. (2010). Expression of class I histone deacetylases during chick and mouse development. *The International Journal of Developmental Biology (54)* , pp. 1527-1537.

Nakagawa, Y., Kuwahara, K., Harada, M., Takahashi, N., Yasuno, S., Adachi, Y., et al. (2006). Class II HDACs mediate CaMK-dependent signaling to NRSF in ventricular myocytes. *Journal of Molecular and Cellular Cardiology (41)* , pp. 1010-1022.

Nambiar, R. M., Ignatius, M. S., & Henion, P. D. (2007). Zebrafish colgate/hdac1 functions in the non-canonical Wnt pathway during axial extension and in Wnt-independent branchiomotor neuron migration. *Mechanisms of Development (124)* , pp. 682-698.

Nervi, C., Borello, U., Fazi, F., Buffa, V., Pelicci, P. G., & Cossu, G. (2001). Inhibiton of histone deacetylase activity by Trichostatin A modulates gene expression during mouse embryogenesis without apparent toxicity. *Cancer Research (61)* , pp. 1247-1249.

Penninckx, F., Cheng, N., Kerremans, R., Van Damme, B., & De Loecker, W. (1983). The effects of different concentrations of glycerol and dimethylsulfoxide on the metabolic activities of kidney slices. *Cryobiology (20)* , pp. 51-60.

Ranhotra, H. S. (2009). Up-regulation of orphan nuclear estrogen-related receptor alpha expression during long-term caloric restriction in mice. *Molecular and Cellular Biochemistry (332)* , pp. 59-65.

Ruthenburg, A. J., Li, H., Patel, D. J., & Allis, C. D. (2007). Multivalent engagement of chromation modifications by linked binding modules. *Nature Reviews Molecular Cell Biology (8)* , pp. 983-994.

Shahbazian, M. D., & Grunstein, M. (2007). Functions of site-specific histone acetylation and deacetylation. *Annual Review of Biochemistry (76)* , pp. 75-100.

Stein, R. A., & McDonnell, D. P. (2006). Estrogen-related receptor alpha as a therapeutic target in cancer. *Endocrine-Related Cancer (13)* , pp. S25-S32.

Strahl, B. D., & Allis, C. D. (2000). The language of covalent histone modifications. *Nature (403)* , pp. 41-45.

Takami, Y., & Nakayama, T. (2000). N-terminal region, C-terminal region, nuclear export signal, and deacetylase activity of histone deacetylase-3 are essential for the viability of the DT40 chicken B cell line. *The Journal of Biological Chemistry (275)* , pp. 16191-16201.

Taunton, J., Hassig, C. A., & Schreiber, S. L. (1996). A mammalian histone deacetylase related to the yeast transcriptional regulator Rpd3p. *Science (272)* , pp. 408-411.

Trivedi, C. M., Luo, Y., Yin, Z., Zhang, M., Zhu, W., Wang, T., et al. (2007). Hdac2 regulates the cardiac hypertrophic response by modulating Gsk3 beta activity. *Nature Medicine (13)* , pp. 324-331.

Trivedi, C. M., Min Lu, M., Wang, Q., & Epstein, J. A. (2008). Transgenic overexpression of Hdac3 in the heart produces increased postnatal cardiac myocyte proloferation but does not induce hypertrophy. *The Journal of Biological Chemistry (283)* , pp. 26484-26489.

Van den Wyngaert, I., De Vries, W., Kremer, A., Neefs, J. M., Verhasselt, P., Luyten, W. H., et al. (2000). Cloning and characterization of human histone deacetylase 8. *FEBS Letters (478)* , pp. 77-83.

Waltregny, D., De Leval, L., Glénisson, W., Ly Tran, S., North, B. J., Bellahcène, A., et al. (2004). Expression of histone deacetylase 8, a class I histone deacetylase, is restricted to cells showing smooth muscle differentiation in normal human tissues. *American Journal of Pathology (165)* , pp. 553-564.

Watanabe, E., Sudo, R., Takahashi, M., & Hayashi, M. (2000). Evaluation of absorbability of poorly water-soluble drugs: validity of the use of additives. *Biological & Pharmaceutical Bulletin (23)* , pp. 838-843.

Wilson, B. J., Temblay, A. M., Deblois, G., Sylvain-Drolet, G., & Giguère, V. (2010). An acetylation switch modulates the transcriptional activity of estrogen-related receptor alpha. *Molecular Endocrinology (24)* , pp. 1349-1358.

Yang, W. M., Tsai, S. C., Wen, Y. D., Fejér, G., & Seto, E. (2002). Functional domains of histone deacetylase-3. *The Journal of Biological Chemistry (277)* , pp. 9447-9454.

Yang, X. J., & Seto, E. (2008). The Rpd3/Hda1 family of lysine deacetylases: from bacteria and yeast to mice and men. *Nature Reviews Molecular Cell Biology (9)* , pp. 206-218.

Yoshida, M., & Beppu, T. (1988). Reversible arrest of proliferation of rat 3Y1 fibroblasts in both the G1 and G2 phases by Trichostatin A. *Experimental Cell Research (177)* , pp. 122-131.

Yoshida, M., Kijima, M., Akita, M., & Beppu, T. (1990). Potent and specific inhibition of mammalian histone deacetylase both in vivo and in vitro by Trichostatin A. *The Journal of Biological Chemistry (265)* , pp. 17174-17179.

Youn, H. D., & Liu, J. O. (2000). Cabin 1 represses MEF2-dependent Nur77 expression and T cell apoptosis by controlling association of histone deacetylases and acetylases with MEF2. *Immunity (13)*, pp. 85-94.

Zeng, F., Baldwin, D. A., & Schultz, R. M. (2004). Transcript profiling during preimplantation mouse development. *Developmental Biology (272)* , pp. 483-496.

Zhang, C. L., McKinsey, T. A., Chang, S., Antos, C. L., Hill, J. A., & Olson, E. N. (2002). Class II histone deacetylases act as signal-responsive repressors of cardiac hypertrophy. *Cell (110)* , pp. 479-488.

Zhao, W., Dai, F., Bonafede, A., Schäfer, S., Jung, M., Yusuf, F., et al. (published online 2009, January 16). Histone deacetylase inhibitor, Trichostatin A, affects gene expression patterns during morphogenesis of chicken limb buds in vivo. *Cells Tissues Organs* , pp. 1-14.

Zupkovitz, G., Tischler, J., Posch, M., Sadzak, I., Ramsauer, K., Egger, G., et al. (2006). Negative and positive regulation of gene expression by mouse histone deacetylase 1. *Molecular and Cellular Biology (26)* , pp. 7913-7928.

Appendix

CURRICULUM VITAE

Personal data

Name:	Claudia Engelmaier
Address:	Passauer Platz 5/3/24 1010 Vienna
Telephone:	+43 676/ 75 82 558
E-Mail:	claudia.engelmaier@gmail.com
Nationality:	Austria
Date of birth:	03.02.1982

Education

2004-date	Study of Biology, University of Vienna Branch of study: Anthropology Field of specialization: Human genetics
2001-2003	Kindergarten teacher education, Kolleg for kindergarten education Albertgasse, Vienna Title of qualification awarded: Certified kindergarten teacher
2000-2001	Primary school teacher education (incomplete), Pädagogische Akademie Krems/Donau
1996-2000	Oberstufenrealgymnasium der Englischen Fräulein Krems/Donau Title of qualification awarded: Matura (A-levels)

Work experience

05/09-07/11	Diploma thesis Center for Anatomy und Cell Biology Department for Cell and Developmental Biology Medical University of Vienna
11/08-01/09	Laboratory course in Molecular Medicine (part 1 and 2; offered by the University of Vienna) Max F. Perutz Laboratories (Assisting with a project: Apolipoprotein B)

07/2008	Internship at the Medical University of Vienna Center for Anatomy und Cell Biology Department for Cell and Developmental Biology (Project in developmental biology: Influence of histone deacetylases on limb development of chicken embryos)
04/06-07/11	Minor employment at Wiener Kinderfreunde, Vienna (After school care of primary school children: assisting with homework)
Summers 08-10	Substitute kindergarten teacher at Wiener Kinderfreunde, Vienna (Child care)
11-12/2007	Minor employment at Holzer Papier Inh. Koch GesmbH, Vienna (Sale, customer care)
08/2007	Call Center Agent at Competence Call Center, Vienna (Inbound: customer care)
11/05-04/06	Minor employment at the medical laboratory Dr. Dieter Kosak, Vienna (Laboratory assistant)
11/04-10/05	Minor employment at Esprit Store, Vienna (Sale, customer care)
10/04-01/05	Minor employment at Kinder in Wien, Vienna (Substitute kindergarten teacher)
08/03-08/04	Kindergarten teacher at Wiener Kinderfreunden and at Kinder in Wien, respectively, Vienna (Child care)

Languages

Mother tongue:	German
Additional languages:	English (Certificate of Advanced English (CAE): Examination in dec. 2004)
	French (4 years of courses in Oberstufenrealgymnasium)

LEBENSLAUF

Persönliche Daten

Name:	Claudia Engelmaier
Adresse:	Passauer Platz 5/3/24 1010 Wien
Telefon:	+43 676/ 75 82 558
E-Mail:	claudia.engelmaier@gmail.com
Nationalität:	Österreich
Geburtsdatum:	03.02.1982

Ausbildung

2004-dato	Biologiestudium, Universität Wien Studienzweig: Anthropologie Spezialisierung: Humangenetik
2001-2003	Ausbildung zur Kindergartenpädagogin, Kolleg für Kindergartenpädagogik Albertgasse, Wien Abgeschlossen mit: Diplom für Kindergartenpädagogik
2000-2001	Ausbildung zur Volksschullehrerin (nicht abgeschlossen), Pädagogische Akademie Krems/Donau
1996-2000	Oberstufenrealgymnasium der Englischen Fräulein Krems/Donau Abgeschlossen mit: Matura (AHS)

Berufserfahrung

05/09-07/11	Diplomarbeit Zentrum für Anatomie und Zellbiologie Abteilung für Zell- und Entwicklungsbiologie Medizinische Universität Wien
11/08-01/09	Wahlbeispiel Molekulare Medizin (Teil 1 und 2; angeboten von der Universität Wien) Max F. Perutz Laboratories (Projektmitarbeit: Apolipoprotein B)

07/2008	Praktikum an der Medizinischen Universität Wien Zentrum für Anatomie und Zellbiologie Abteilung für Zell- und Entwicklungsbiologie (Entwicklungsbiologisches Projekt: Einfluss von Histondeacetylasen auf die Extremitätenentwicklung bei Hühnerembryonen)
04/06-07/11	Geringfügige Beschäftigung bei den Wiener Kinderfreunden, Wien (Nachmittagsbetreuung von Volksschülern: Lernstundenhilfe)
Sommer 08-10	Aushilfskindergärtnerin bei den Wiener Kinderfreunden, Wien (Kinderbetreuung)
11-12/2007	Geringfügige Beschäftigung bei der Holzer Papier Inh. Koch GesmbH, Wien (Verkauf, Kundenbetreuung)
08/2007	Call Center Agent im Competence Call Center, Wien (Inbound: Kundenbetreuung)
11/05-04/06	Geringfügige Beschäftigung im Medizinischen Labor Dr. Dieter Kosak, Wien (Laborassistentin)
11/04-10/05	Geringfügige Beschäftigung im Esprit Store, Wien (Verkauf, Kundenbetreuung)
10/04-01/05	Geringfügige Beschäftigung bei Kinder in Wien, Wien (Aushilfskindergärtnerin)
08/03-08/04	Kindergartenpädagogin bei den Wiener Kinderfreunden bzw. bei Kinder in Wien, Wien (Kinderbetreuung)

Sprachkenntnisse

Muttersprache:	Deutsch
Erworbene Sprachen:	Englisch (Certificate of Advanced English (CAE): Absolvierung der Prüfung im Dez. 2004)
	Französisch (4 Jahre Schulkenntnisse: Gymnasium)

Eidesstattliche Erklärung

Ich, Claudia Engelmaier, erkläre, dass die vorliegende Diplomarbeit von mir selbst verfasst wurde und ich keine anderen als die angeführten Behelfe verwendet bzw. mich auch sonst keiner unerlaubten Hilfe bedient habe.

Ich versichere, dass ich dieses Diplomarbeitsthema bisher weder im In- noch im Ausland (einer Beurteilerin/einem Beurteiler zur Begutachtung) in irgendeiner Form als Prüfungsarbeit vorgelegt habe.

Weiters versichere ich, dass die von mir eingereichten Exemplare (ausgedruckt und elektronisch) identisch sind.

Wien, im Juni 2011 Unterschrift:.....